ΠΑΝΕΠΙΣΤΗΜΙΟ ΚΡΗΤΗΣ
ΤΜΗΜΑ ΧΗΜΕΙΑΣ

ΜΕΤΑΠΤΥΧΙΑΚΟ ΠΡΟΓΡΑΜΜΑ ΕΦΗΡΜΟΣΜΕΝΗΣ ΜΟΡΙΑΚΗΣ ΦΑΣΜΑΤΟΣΚΟΠΙΑΣ

ΜΕΤΑΠΤΥΧΙΑΚΗ ΕΡΓΑΣΙΑ

"Μελέτη της αντιστρεπτής απόκρισης φωτοχρωμικών πολυμερών στην ακτινοβολία λέϊζερ και εφαρμογές τους ως 'έξυπνα' συστήματα αισθητήρων και διακοπτών."

ΛΑΚΙΩΤΑΚΗ ΚΛΕΑΝΘΗ

ΔΕΚΕΜΒΡΙΟΣ 2004

ΗΡΑΚΛΕΙΟ ΚΡΗΤΗΣ

UNIVERSITY OF CRETE
CHEMISTRY DEPARTMENT

POSTGRADUATE PROGRAMME IN APPLIED MOLECULAR SPECTROSCOPY

MASTER THESIS

"Study of the reversible response of photochromic polymers to laser irradiation and applications as "smart surfaces", sensors and switches"

LAKIOTAKI KLEANTHI

DECEMBER 2004

IRAKLION CRETE

Contents

Introduction

The word “nanotechnology” was coined independently in the 1980s, first by Norio Taniguchi and then by K Eric Drexler. Taniguchi approached it from the viewpoint of a precision engineer, noting that novel techniques would be needed to meet technological demands. Essentially, his definition includes all technologies that involve either a critical dimension or a critical tolerance of below 100 nanometres. Drexler approached it as a physicist and broadly defines nanotechnology as concerned with the manipulation of matter at the nanometre scale.

Nanotechnology is intrinsically multidisciplinary, reliant on the basic science, analytical techniques and methodologies of a number of disciplines including: chemistry, physics, electrical engineering, materials science and molecular biology. Although nanoscience might simply be seen as a natural and necessary progression from the (sub) micron-scale engineering that has driven the microelectronics and computing industries thus far, it is not only the trend towards higher levels of miniaturization but the wealth of novel physical, chemical and biological behavior that occurs on the nanometre scale that makes nanoscience such a fundamentally exciting and technologically relevant area of research.

Understanding of new materials at the molecular level has become increasingly critical for a new generation of nanomaterials for nanotechnology, namely, the design, synthesis, and fabrication of nanodevices at the molecular scale. Not only the way they are composed but also the way they behave becomes essential in order for them to become applicable.

In engineering and applied science, important areas for research are new sensors, actuators, switches, as well as mechanisms efficient for their manipulation and fine control. The field of research is highly multi-disciplinary, combining medicine and biology as applications supported by traditional areas of engineering, computer science, physics and biochemistry.

Richard Feynman delivered a speech in 1960, “There’s Plenty of Room at the Bottom,” which envisioned a technological world of the very small, where the units of construction were not blocks or circuits but atoms. Miniaturization will extend to mechanics and electronics. The grouping of these two fields leads to the development of microelectromechanical systems known as MEMS.

To date, the mechanical actuation of movable microcomponents in MEMS is performed using electrical energy. Nevertheless, to avoid the wiring with external electronics, optical manipulation of such components seems very promising. Highly directional laser beams can access and manipulate the MEMS components with great accuracy even in nanoscale dimensions. For this reason we have extensively investigated a novel molecular substrate which can operate as a laser driven photoswitch. The substrate consists of a polymer matrix doped with photochromic molecules. Due to the rapid and reversible transformation that occurs in the photochromic molecules the above mentioned requirements of micro-nanotechnology are satisfied by the use of such reversibly responsive molecules as functional materials.

The substrate demonstrated in this thesis consists of a polymer matrix doped with photochromic Spiropyran molecules. Alternating irradiation by laser beams of different wavelengths fully controls the operation of this photoswitch. The reversible actuation of the examined substrate is based on the phenomenon of photochromism. In particular the property of the photochromic molecules to interconvert between different geometrical forms (isomers) upon irradiation is responsible for the reverse mechanical effect. The extensive use of polymers in the technology of integrated circuits and MEMS makes the particular polymeric photoswitch a promising candidate for microsensors, microactuators and micro optics devices.

1
Photochromism

1.1 General definitions

"Photochromism" is simply defined as a *light-induced reversible change of color*. It has become a common name because many people wear photochromic glasses that darken in the sun and recover their transparency in diffuse light. The first commercial spectacles were made of glass lenses doped with inorganic (mainly silver) salts but in recent years, organic photochromic lenses, which are lighter and therefore more comfortable to wear despite their limited lifetime, have made an important breakthrough in the world market. Moreover, the fact that some chemical species can undergo reversible photochemical reactions goes beyond the domain of variable optical transmission and includes a number of reversible physical phenomena such as optical memories and switches, variable electrical current, ion transport through membranes, variable wettability, etc. For this

purpose, organic photochromic compounds are often incorporated in polymers, liquid crystalline materials, or other matrices.

A photochromic compound is one that undergoes a reversible change upon irradiation. For example, if the compound has an 'A' form (usually pale or colourless), on irradiation with UV or visible light changes to a more deeply coloured 'B' form. The reverse reaction, 'fading', may occur thermally at room temperature or by heating. In principle, it can be repeated many times but 'fatigue' may occur.

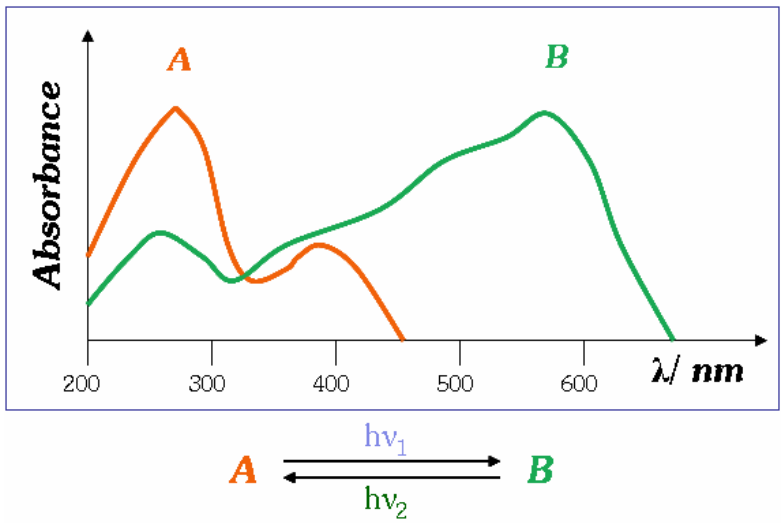

Figure 1.1: Reversible change in the absorption spectrum of a photochromic compound upon appropriate irradiation.

Interest in photochromism was continuous but limited until the 1940–1960 period, which saw an increase of mechanistic and synthetic studies, particularly in the research groups of Hirshberg and Fischer in Israel [1]. In 1950, Hirshberg suggested the term "photochromism" [from the Greek words: *phos* (light) and *chroma* (color)] to describe the phenomenon. This is the name used today. However, it is not limited to colored compounds; it applies to systems absorbing from the far UV to the IR, and to very rapid or very slow reactions.

Photochromism expanded during the 1960s in parallel with the development of physical methods (IR, NMR, X-ray, UV, time-resolved and flash spectroscopy) and organic synthesis. Applications, such as the photochromic micro image (PCMI) process, which showed the possibility of reducing the 1245 pages of a

Bible to about 6 cm^2, attracted considerable interest. An important book was published in 1971 [2]. However, it appeared that the photodegradation of the known families of organic photochromes limited their potential for applications [3-7].

A revival of activity started in the 1980s, essentially because of the development of fatigue-resistant *spirooxazine* and *chromene* derivatives. They triggered the fabrication and commercial application of photochromic ophthalmic lenses. Since then, other commercial systems have been developed, and new photochromic systems have been discovered and explored.

Photochromism as mentioned above is a reversible transformation of a chemical species induced in one or both directions by absorption of electromagnetic radiation between two forms, A and B, having different absorption spectra [4].

As for organic photochromic molecules, the reactant is generally colorless, meaning that its electronic absorption starts only from the UV region (< 350 nm), while the products induced by the UV irradiation show the intense absorption in the visible region (400 to 700 nm). This behavior indicates that the isolated π-electron systems in the reactant become extensively conjugated in the products. Changes in other molecular properties such as reflective and dielectric constants can also occur along with the color change during the photochromic reaction. Reversibility is the main criterion for photochromism. The back reaction is induced mostly by a thermal mechanism (*Photochromism of type T*) at room temperature, while some photochromic molecules yield thermally stable photoproducts. For such systems, back reactions are photochemical (*Photochromism of type P*).

The most prevalent organic photochromic systems involve *unimolecular* reactions. The most common photochromic molecules have a colorless or pale yellow form A and a colored form B (e.g., red or blue). This phenomenon is referred to as *positive photochromism*. Other systems are *bimolecular*, such as those involving photocycloaddition reactions. When $\lambda_{max}(A)>\lambda_{max}(B)$, *photochromism* is *negative* or *inverse* [4].

The unimolecular processes are encountered, for example, with *spiropyrans*, a family of molecules that has been studied extensively. Solid photochromic spiropyrans or solutions (in ethanol, toluene, ether, ketones, esters, etc.) are

colorless or weakly colored. Upon UV irradiation, they become colored. The colored solutions fade *thermally* to their original state; in many cases, they can also be decolorized (*bleached*) by visible light. A few spiropyrans display negative photochromism. They are colored in the dark and *bleached* by UV light. Many spiropyrans are also *thermochromic*, and spectra of the colored forms are identical to those produced photochemically.

1.2 Process of photochromism. One-photon and two-photon systems

In general, the photochromic processes involve a one-photon mechanism. B is formed from the singlet (^{1}A*) or triplet (^{3}A*) excited states or both. B, the photoproduct, may also be formed from an upper excited state populated by absorption of two photons.

The transition probability to populate the final state (hence to obtain the photoproduct) depends on the product of the photon irradiances Ep(1) and Ep(2) of the two exciting beams.

It is, therefore, advantageous to utilize lasers emitting high photon irradiance, such as those generating picosecond or subpicosecond pulses. Two absorption processes may be distinguished:

a) simultaneous absorption of two photons via a virtual level.

b) sequential two-photon absorption where the second photon absorption takes place from a real level.

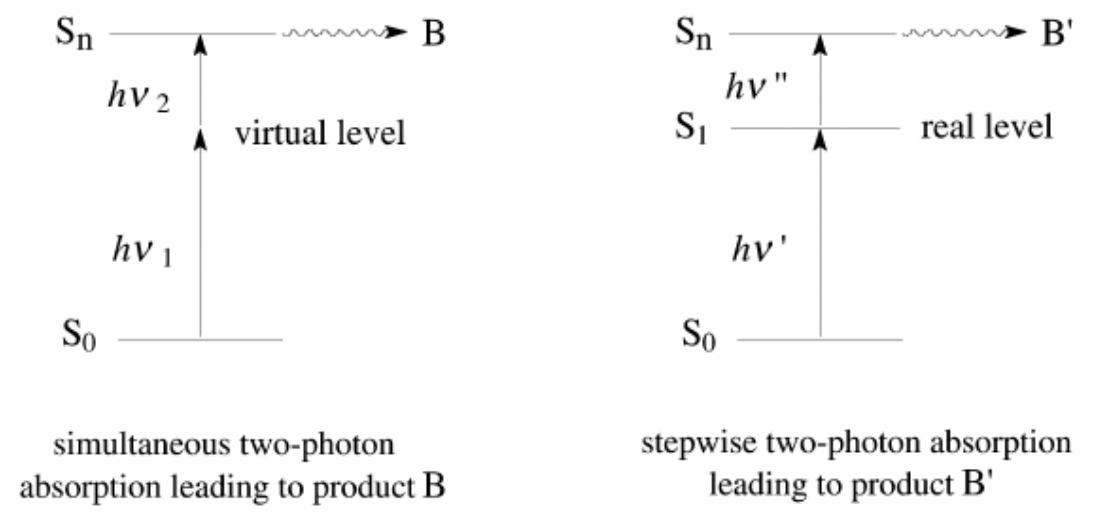

Figure 1.2: Process of photochromism

The simultaneous process has been successfully used for exciting photochromic molecules at specific positions inside a volume for 3D memory systems (writing process). A two-photon absorption process was also used to excite the written molecules that emit fluorescence (reading process) [5,6,8,9].

The medium in which the photochromic compound is incorporated plays also an important role. It can strongly influence or control the kinetics of the thermal back reaction when it occurs, the color of the species formed in the forward photochemical reaction, and other properties of the photochromic process.

1.3 Applications of photochromism

Photochromism and its various characteristics can also be defined according to the type of application at which they are targeted. Two general types of applications can be defined:

Applications directly depended upon the color change caused by the molecular and electronic structures of the two species (A, B) and their corresponding absorption or emission spectra.

Examples of the above category are:

- Variable-transmission optical materials such as the photochromic ophthalmic lenses or camera filters;
- Fluid flow visualization;
- Optical information storage
- Novelty items (toys, T-shirts, e.t.c.);
- Authentication systems (security printing inks);
- Cosmetics

Applications depended upon changes in the physical or chemical properties that occur along with the more easily observed color change during the photochromic reaction.

Examples of such properties are conductivity, refractive index, dipole moment, dielectric constant, chelate formation, ion dissociation, phase transitions, solubility and viscosity. Certain physical changes (e.g. volume change) that occur when the photochromic entity is chemically attached to the macromolecular backbone of polymers are of special interest and are examined analytically in the present work.

Some examples of potential applications utilizing the physical or chemical changes that accompany the observed shift in the absorption maxima are:

- Optoelectronic systems (semi-conductors modulated by photochromic pigments);
- Reversible holographic systems;
- Optical switches;
- Optical information storage;
- Photochemically switchable enzymatic systems;
- Nonlinear optical devices;
- Responsive polymer surfaces;

Of all these potential applications, a few have been commercially successful (polymer based photochromic eyewear, novelty items and security printing inks) or demonstrated to be useful (fluid flow visualization). Several others have shown considerable promise and may very well be utilized in commercial products in the future.

2

The Spiropyran family

2.1 Structure and characteristics

Spiropyrans and their analogues have been extensively studied since the pioneering work by Fisher and Hirshberg in 1952 [1]. Spiropyrans consist of a pyran moiety and another moiety containing conjugated rings that are held orthogonal by a common spiro-carbon atom. Spiropyrans refers in general to a substituted 2H-pyran having a second ring system, usually heterocyclic, attached to the 2-carbon atom of the pyran in a spiro manner as shown in figure 2.1. For example a carbon atom is common to both rings. The pyran portion of spiropyran usually refers to 2H-1-benzopyran, as well as to its literal meaning of a single ring. In literature is often used the 'spirochromene', incorporating the common name for [2H]-1-benzopyran. The compound from different heterocycles having the names 'A' and 'B' and where the shared carbon atom would be numbered 'x' in heterocycle 'A' and 'y' in heterocycle 'B', should be named 'spiro(A-x,y'-B),'

with the names in alphabetical order and the second name bearing the primed numbers; thus, spiro(2H-1-benzopyran-2,2'-2H-indole) [7]. A simpler name such as '**indolinospiropyran'** is easily understood and often used informally as a general term.

A very wide variety of possible spiropyran ring systems is implied by the above definition, and a considerable number of these systems have been prepared and examined for use in various practical applications. The spiropyrans, their photochromism, and their applications have been extensively reviewed [8].

Reversible photocoloration is attributed to equilibrium between the spiropyran (closed, colorless) form and a merocyanine (open, colored) form, as shown in figure 2.1 for an indolinospirobenzopyran. The merocyanine is an equilibrium mixture of geometrical conformations and its electronic distribution varies from highly zwitterionic to an essentially nonionic ortho-quinoidal structure.

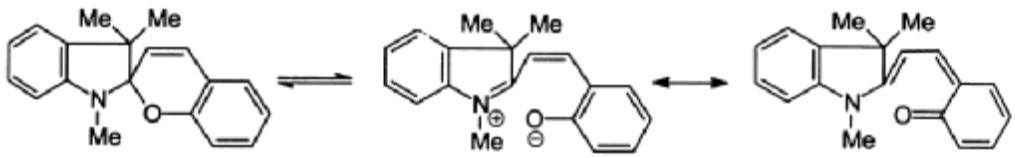

Figure 2.1: Spiropyran and open merocyanine forms

The way in which authors consider these compounds seems to be influenced by the synthetic route the used. If an active methyl group is condensed with a hydroxyaldehyde compound, it is a spiropyran; if the same compound is made by condensing a formylmethylene group with a ketomethylene, it is a merocyanine, because these are the respective traditional synthetic routes.

The existence of the spiropyran-merocyanine equilibrium implies that in principle a dimethinemerocyanine could be closed to a pyran isomer, thus exhibiting 'reverse' photochromism (bleaching with visible light and thermally recoloring in the dark), but no systematic study of this large class of dyes appears to have been carried out. However, many merocyanines can be irreversibly photobleached by reaction with some added reagent.

Applications of spiropyran molecules cover a wide range of scientific interest. Biological applications of spiropyrans incorporated into membranes and their use as specific ion recognition sensors and signal transducers as well as spiropyran-modified artificial monolayer, bilayer, and multilayer membranes whose physical and chemical properties can be controlled by irradiation have gained a great deal of attention lately.

2.2 Photochromism of Spiropyran

As mentioned above, spiropyrans consist of a pyran moiety and another moiety containing conjugate rings that are held orthogonal by a common spiro-carbon atom. Since both the constituent π-electron systems do not interact significantly in the spiro form, the absorption spectrum of the spiropyran molecule is approximately reproduced by the superposition of the spectra of the two individual moieties [9]. Hence the spiropyran is generally colorless. The photochromic process in spiropyrans features the dissociation of the bond between the spiro carbon and the oxygen, producing a distribution of isomeric open forms (merocyanines), which are revertible to the original closed form (Figure 2.1.1).

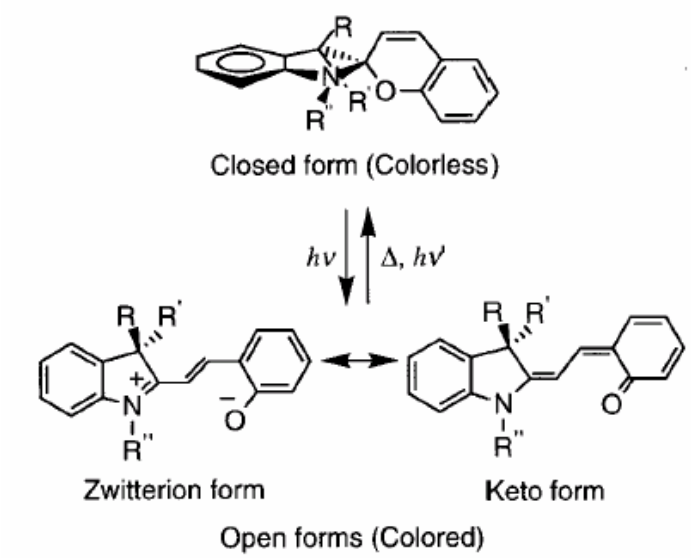

Figure 2.2.1: Closed and open forms of Spiropyran

Extensive conjugation of the π-electron system in the open form leads to the appearance of the strong absorption in the visible region where the closed form does not absorb. Most of the colored open forms are thermally unstable; the lifetime depends on the properties of the solvent, the subsistent in the benzopyran ring, and the temperature. With absorption of light in the visible region, the open forms can also revert back to the original spiro form. The photochromic reactions of spiropyrans and their analogues have been examined with continuous absorption spectroscopy [10], transient absorption spectroscopy [11], and transient Raman spectroscopy [12].

Owing to the difficulties in the assignment of the open forms involved, however, the detailed dynamics of spiropyran materials have not been clarified. Their structural features arise from the hetero atoms included and the complicated molecular structure arising from the fact that the open forms can take the keto, zwitterion, and hybrid forms [10], and that the open forms can take a number of stereoisomeric configurations with respect to the carbon-carbon bonds [13]. It has been known that only 2H-benzopyrans (chromenes) and their analogues, which constitute the spiropyran molecules as the pyran moiety, also show photochromic behavior on UV irradiation. Recently, much attention has been paid to the photochromism of 2H-benzopyrans. Furthermore, this photochromism is also important for the detailed understanding of the ring-opening reactions of spiropyrans. This is because, for the assignment of the open forms from 2H-benzopyrans, the three structures (keto, zwitterion, and hybrid) caused by the two hetero atoms do not need to be taken into consideration. Since the C–O bond cleavage of spiropyrans is initiated with absorption of light in the UV region where the benzopyran moiety absorbs, the photochromism of 2H-benzopyrans can be treated as the simplified model for that of spiropyrans [14].

As previous reported UV excitation of BIPS (and of other spiropyrans) leads to a heterolytic cleavage of the bond between the spiro carbon atom and the oxygen atom. The molecule can now unfold, the two parts of the molecule are allowed to rotate relative to each other, and thus an extended, more planar configuration is attained. Now the π-electrons conjugate across the entire structure (which may be classed among the merocyanine dyes) resulting in an intense absorption in the range ***500-600*** nm. The merocyanine form of BIPS and its visible

absorption spectrum are also shown in figure 2.2.2**.** In a subsequent thermal back reaction, the photochemically induced color usually fades on a time scale of seconds to minutes (at room temperature), as the merocyanine form reverts to the thermodynamically more stable spiro form of the molecule [13].

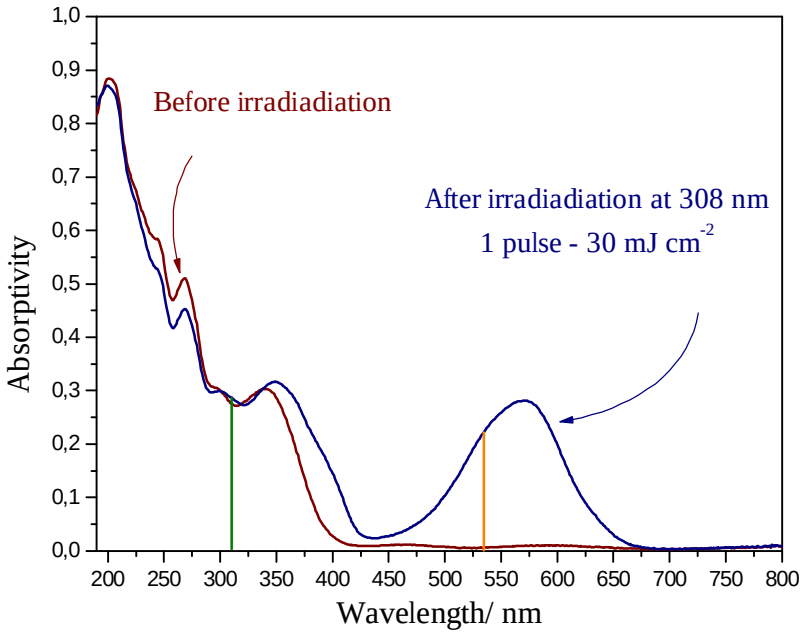

Figure 2.2.2: Absorption spectrum of 5%Spiropyranin 955 PEMMA before and after UV irradiation.

2.3 Existence of Several Merocyanine Isomers.

The open, merocyanine form of the spiropyran molecule possesses a central chain of three carbon-carbon bonds, C_2-C_3-C_4-C_{4a} (Figure 2.3.1) [13]. Any geometric arrangement of this chain may be described by three associated dihedral angles. In the electronic ground state, the merocyanine-like molecular structure confers partial double-bond character to each of the bonds of the central chain. Therefore each dihedral angle will be close to either 0**º** or 180**º,** corresponding to either a cisoid or a transoid configuration of the particular chain segment. So in principle there should be 2^3 = 8 possible overall configurations. It has been recognized early on that of the eight possible overall configurations, only those that have a central transoid segment represent a local energy minimum and hence a

stable merocyanine isomer, while the other, near-planar configurations with a central cisoid segment are raised in energy because of internal steric hindrance [39].

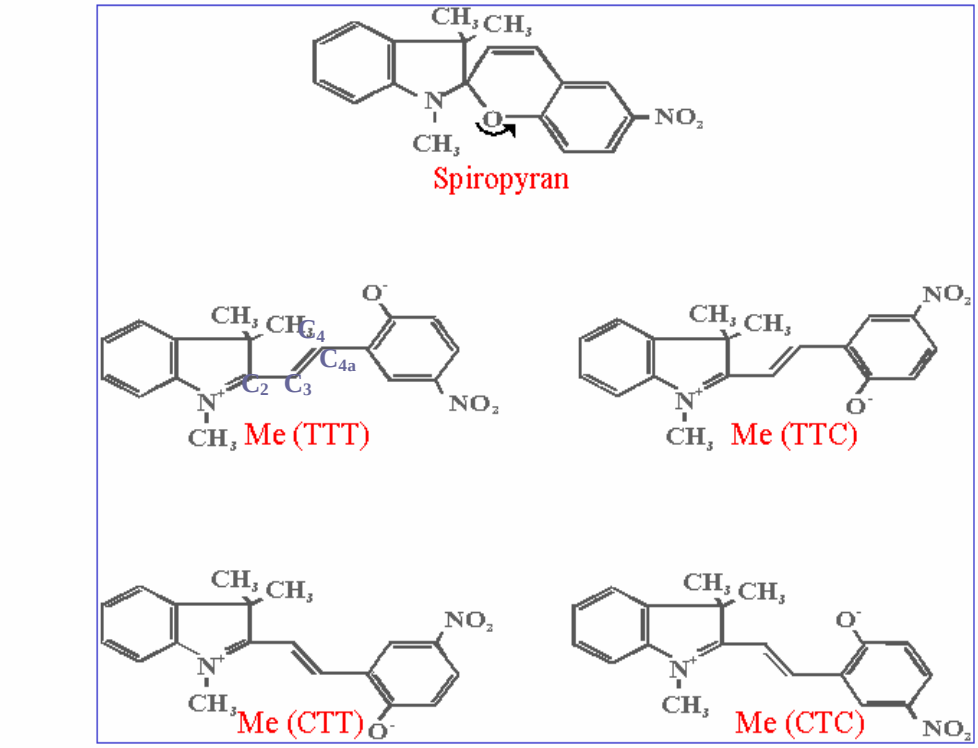

Figure 2.3.1: Spiropyran and the four transoid merocyanine forms.

The above verification has been corroborated by semiempirical calculations [15]. In addition to the four transoid forms, a fifth cisoid isomer "CCT" is predicted, which, however, has a highly twisted central bond (θ= 60°) and which is separated from the energetically more favorable CTT form only by a small energy barrier [13]. Experimental proof for the existence of several merocyanine isomers was obtained when the photochemical spiropyran-merocyanine conversion was carried out in rigid media at low temperature [39, 40]. Merocyanine isomers may also be distinguished by their luminescence properties [30]; they have been further characterized by resonance Raman spectra in various solvents [41]. For nitro-substituted spiropyrans, merocyanine isomers may be precipitated in aliphatic solvents; thus the molecular structure of TTC isomers from several spiropyrans could be determined [42]. Further evidence for the existence of several

merocyanine isomers comes from the thermal fading of the photochromic color, i.e., from the kinetics of ring-closure in the electronic ground state. In alcoholic solvents, monoexponential decay is found throughout, indicating fast equilibration of the isomers prior and during the slower ring closure. However in aliphatic solvents, biexponential decay may be observed [39,40]. This can be understood if the rates of interconversion between the open isomers are of a magnitude comparable to the rate of the ring-closure from one particular isomer.

2.4 Pathways for the photochemical ring opening of 6-NO_2-BIPS

Görner [21] used nanosecond flash photolysis to study the properties of the 6-nitro-indolinobenzopyran. His work was focused on the photochemistry of the spiropyran in its merocyanine forms which are present at room temperature as one (intermediate) cis isomer and one (stable) trans isomer. The trans→cis photoisomerization is suggested to occur mainly via a singlet mechanism. The nitro group is proposed to enhance the quantum yield of intersystem crossing in the Sp form.

Spectroscopic and kinetic results with ~ 15 ns time resolution for the nitro-substituted spiropyran in solution at room temperature indicate just four species, (i) Sp, (ii) trans, (iii) cis and (iv) a triplet state [22]. Once the observed cis isomer is photo-chemically generated either from ^{1}Sp* or ^{1} trans*, it converts into the trans isomer. Görner strongly suggested a barrier between the two observable isomers and a higher energy content of cis with respect to the trans isomer. He proposed that the potential energy surface of the ground state, along with the reaction coordinate, should have at least two maxima, whereby that (Esp) between the spiropyran and the cis isomer should be significantly larger than that (Ec-t) between the cis and the trans isomers (Figure 2.4.1).

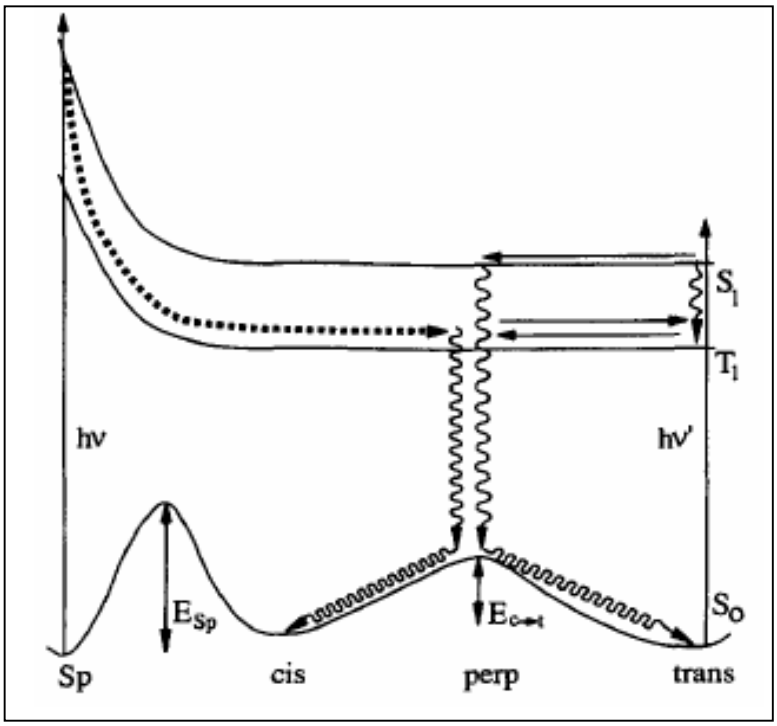

Figure 2.4.1: pathways fort he photochemical ring opening of the 6-NO_2-BIPS

The absence of fluorescence from the closed form indicates either efficient intersystem crossing from ^{1}Sp* or rapid geometrical changes due to ring opening.

Two routes account for the intermediacy of the ^{3}trans* state in the photocoloration process: (a) intersystem crossing in the spiropyran geometry followed by ring opening and (b) first ring opening in the S_1 state and then intersystem crossing in the merocyanine moiety. The essential features of the proposed model are: (1) A triplet route account for the photocoloration of the compounds. The main effect of the nitro group is intersystem crossing at the Sp moiety; the cis and trans ground states are populated by a second intersystem crossing step (at the perpendicular geometry, involving the ^{3}perp* $\rightleftarrows$ ^{3}trans, equilibrium). (2) The main pathway of trans ~ cis photoisomerization occurs in singlet states:

^{1}trans* $\rightarrow$ ^{1}perp* $\rightarrow$ perp $\rightarrow$ β cis + (1 – β) trans.

Here, β is the fraction of ^{1}perp* decaying into the cis isomer. Formation of the observed ^{3}trans* triplet state of the compound is only a side reaction, supported by the relatively small triplet yield upon excitation at 530 nm [15]. (3) Pathways

via excited singlet or triplet states, depending on the absorbing species, lead both to cis, the triplet pathway from Sp and the singlet pathway from trans.

Studies were performed by nanosecond laser photolysis in solutions from Chibisov and Görner [22]. An intermediate, which is attributed to a photoisomer with cis structure, was observed upon excitation of either the spiropyran form or the trans isomer. The merocyanine form of nitro-substituted spirobenzopyrans was found to exhibit fluorescence at room temperature and phosphorescence at -196 °C [23]. The specificity of the photoprocesses for a particular indoline merocyanine might be caused by the existence of several transoid isomers that convert sequentially into the most stable one [13]. Another peculiarity of merocyanines is the ability to form dimers and higher stoichiometry aggregates [18]. Besides, a better understanding of the photoprocesses of the merocyanine form(s) should be helpful for increasing the fatigue resistance of spiropyrans.

2.5 Pathways for the isomerization of 6-NO_2-BIPS

The back reaction of merocyanine to the colourless spiro isomer form proceeds photochemically as well as thermally. Thermal isomerization takes place at room temperature, and the reaction kinetics have been extensively studied in various matrices [16]. Abe et al [15] carried out semiempirical calculations on the reaction coordinate of the conformational changes between the merocyanine-form isomers to reveal the pathways for the spiropyran to merocyanine transformation. Abe concluded that all of the merocyanine-form isomers (four conformers) are less stable by as much as 32.03-46.85 kJ mol^{-1} than the spiro-form isomer. Of the four conformers, the most stable is TTT form, the next is the CTT and the most unstable form is the CTC. By calculating the energy profiles of the isomerization processes he concluded that (a) the TTT$\rightleftharpoons$TTC process is allowed from both directions (b) the TTT$\rightleftharpoons$CTT process is prohibited due to discontinuities in the potential energy

surface. (c) the TTC⟹CTC process is allowed from both directions and (d) the process CTT⟹CTC is also allowed from both directions.

Although it requires various types of spin correlations, symmetry considerations and so on to judge whether or not real bond formation takes place, a smooth potential energy curve without a discontinuity is a necessary condition for cyclization to take place.

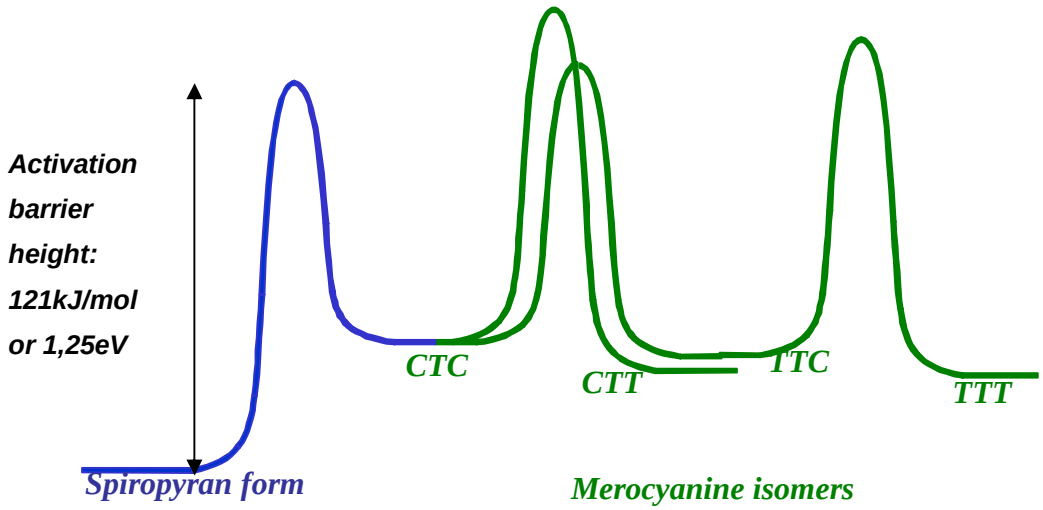

Figure 2.5.1: Pathways for the isomerization of 6-NO_2-BIPS

Cyclization from the CTC conformation satisfies the minimum requirement. In all cases, the potential energy curves showed a discontinuity. The discontinuities indicate that direct single-step conversion from the TTC, CTT or TTT conformers to the spiro-form isomer is prohibited. Careful examination of the potential energy curves reveals that the discontinuities are due to channel routes to other conformations, namely from TTC to CTC and from CTT to CTC. In the case of the TTT conformer, two conformational changes from TTT to TTC and TTC to CTC are involved.

Of the four conformers of the merocyanine-form isomers, only the CTC conformer was found to cyclize thermally through an appropriate reaction path. Isomerization from TTC to CTC is necessary for the TTC form to cyclize to the spiro-form isomer. Two routes are possible for the isomerization from TTT to CTC. One is via TTC and the other is via CTT. The route via CTT is prohibited.

The fact that only the TTC form has been observed as a merocyanine-form isomer by NMR can be interpreted as follows. Although the TTT conformer has the lowest energy, the large barrier from the TTC to the TTT conformer suppresses population of the TTT conformer. Therefore the TTT conformer is not detected. The CTT conformer is more stable than the TTC conformer, but the population is less than that of the TTC conformer. This is due to the large barrier from the CTC to the CTT conformer as shown in figure 2.5.1. The photogenerated CTC conformer mostly converts to the more stable TTC conformer and other conformers, CTT and TTT, are not populated. This is the reason why the TTC conformer is the dominant merocyanine-form isomer. The thermal cyclization of the TTC conformer is considered to proceed via the CTC conformer.

2.6 Formation of aggregates in 6-NO_2-BIPS

Since the first studies on the photochromism of the spiropyrans, by Fischer et al.[1], a great number of studies have been done on their properties. In the case of the 1,3,3-tri-methyl-6'-nitrospiro[indoline-2,2'[2H]-benzopyran] or else (6'-nitro-BIPS), in aliphatic solvents, photoinduced spontaneous aggregation processes were observed and the aggregates were defined as "quazi-crystals"[16]. A. Kalisky et al. [17] proposed that, in a nonpolar solvent, there was formation of a cisoid ring open photoproduct, denoted **X,** within 8 ps which underwent isomerization to the transoid form, denoted B (Mc), in approximately 300 ps. The formation of the triplet state of the spiropyran, ^{3}Sp, was said to be in competition with the formation of **X.** Aggregation was stated to occur by a bimolecular reaction between ^{3}Sp and a ground-state molecule Sp [17]. However, the latter experiments left unexplored the time range of the first few nanoseconds (1-10 ns).

Lenoble et al [18] gave new insight into the mechanism of photochromism of the 6'-nitro-BIPS since two new transients were discovered in the early nanosecond time domain. The influence of oxygen was shown to be the important factor in elucidating the presence of the new transients. They proposed a more complete mechanism of the process of photochromism unifying results from the early picosecond time domain to the millisecond time domain**.**

By performing microsecond and nanosecond laser flash techniques Lenoble et al have shown that the triplet excited state of the closed spiropyran ^{3}Sp leads to the open cisoid isomer in the triplet excited state ^{3}X. The latter species then reacts with the open transoid form Mc in a bimolecular reaction to form the dimers (maximizing at 630 nm). Moreover, the closed form Sp leads directly to Mc since the rise time of Mc is affected by oxygen (from 10 ns in nitrogen to 22 ns in oxygen). This gives proof of the direct formation of Mc from ^{3}Sp as seen in the sensitization studies in **EPA** and 2MeTHF at -100˚C13 and in polystyrene matrix [19]. The above experimental results are summarized in the following figure 2.4.1.

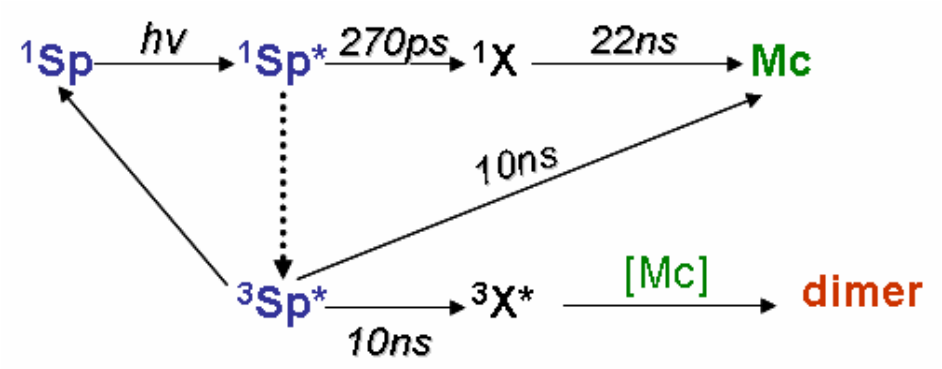

Figure 2.6.1: Recommended durations for the Sp-Mc transformation-Mechanism I

A transient rising in 8ps from 400 to 650 nm was observed by Krysanov et al [20] and assigned to a single species, the open cisoid form, X. According to Lenoble [18], the spectrum of the transient seen in his study clearly shows two maxima at 450 and 580 nm. This result may infer that this spectrum is the result of the superposition of two spectra: (a) a $S_1 \rightarrow S_n$, transition of X or (b) a $T_1 \rightarrow T_n$, transition of ^{3}Sp. Another possibility is that the spectrum is the $S_1 \rightarrow S_n$ absorption spectrum of the spiropyran. The latter possibility is consistent with mechanism proposed above. The former possibility brings a modification to mechanism I and is described below in mechanism II for the photochromism of 6'- nitro-BIPS in nitrogen-degassed aliphatic hydrocarbons:

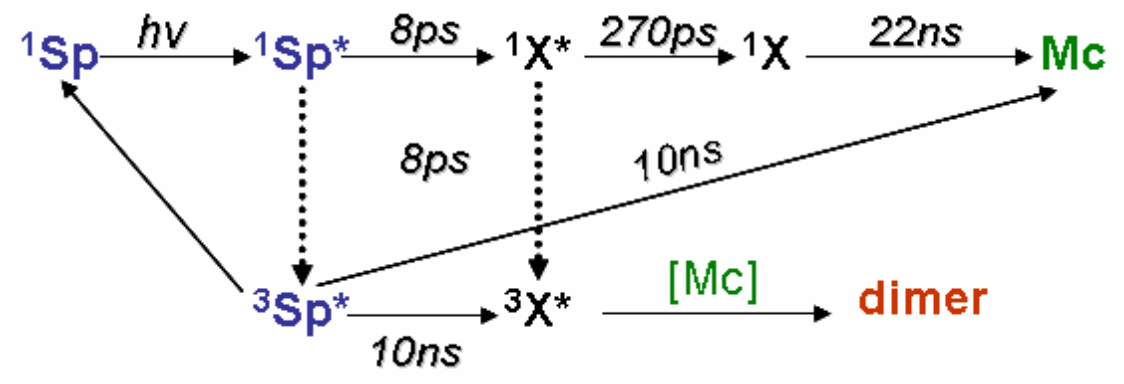

Figure 2.4.2: Recommended durations for the Sp-Mc transformation-Mechanism II

3
Samples preparation

3.1 Film casting

For the preparation of the films used in the bending experiment, solutions of 95.0% of the polymer polyethylmethacrylate-co-methylacrylate (PEMMA) with average molecular weight Mw ~100,000 (Aldrich) and of 5.0% of the photochromic molecule 1',3'-dihydro-1',3',3'-trimethyl-6-nitrospiro [2H-1-benzopyran-2,2'-(2H)-indole] (Aldrich) or else 6-NO_2 BIPS are prepared in toluene. The solutions are undergoing ultra-sonic baths. A certain volume of each solution is cast on a glass substrate using a Pasteur pipette and is allowed to dry in vacuum for 72 h to ensure complete removal of toluene. Toluene as a solvent in ambient conditions is intensively volative therefore fast evaporation would cause inhomogeneities in the surface of the samples. Thus, the drying procedure takes place slowly enough to ensure a uniform surface of the casted film. After drying, the sample is immersed into water, which causes the film to be detached from the substrate and float on the water surface. The freestanding film is then left to dry for

few hours in ambient conditions. The thickness of the films used in different experiments is in the range of 60 to 200 μm and the films are optically thick. Finally each film is cut and then fixed onto a stable support, leaving an area of 1.5×2.5 mm^2 of the film to stand freely.

3.2 Spin coating

For the absorption and wettability measurements the preparation of the films has to be changed due to different experimental requirements. In the absorption experiments the samples have to be optically thin for the reasons mentioned in the theoretical section. As for the wettability measurements, 2000-3000Å thickness of the sample is appropriate for the performance of the experiments. Therefore the spin coating method is used for the samples preparation.

For the spin coating process there are four distinct steps that are followed. Step 3 (flow controlled) and Step 4 (evaporation controlled) are the two stages that have the most impact on final coating thickness. Solutions of 3% by volume are prepared in toluene or in dichloromethane. The concentration of the photochromic dopant in the polymer matrix varies depending on the experiment for which is prepared.

The first step is the deposition of the coating fluid onto the wafer or substrate. In our case a glass Pasteur pipette was used for the deposition of the solution in the glass or quartz substrate. Usually this dispense step provides a substantial excess of coating solution compared to the amount that will ultimately be required in the final coating thickness. Another potentially important issue is whether the solution wets the surface completely during this dispensing stage. If not, then incomplete coverage can result.

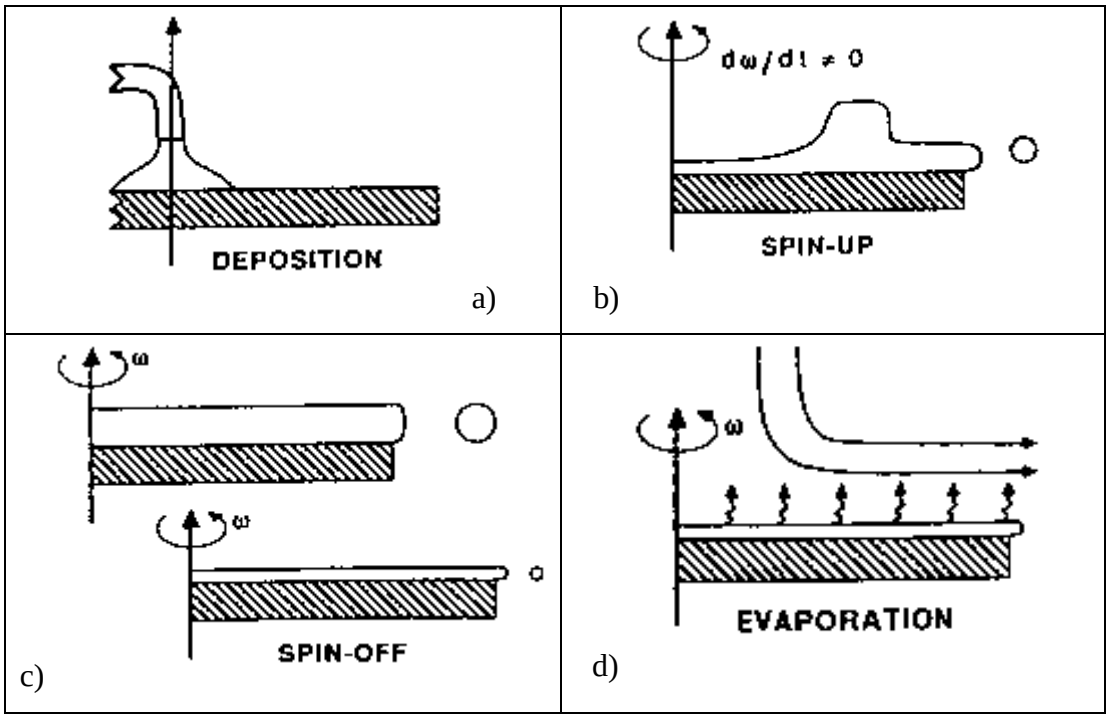

Figure 5.2.1: a)Deposition of the film b) Spinning up of the film c) Spinning off of the film d) Evaporation of the solvent

The second step is when the substrate is accelerated up to its final, desired, rotation speed. This stage is usually characterized by aggressive fluid expulsion from the wafer surface by the rotational motion. Because of the initial depth of fluid on the wafer surface, spiral vortices may briefly be present during this stage; these would form as a result of the twisting motion caused by the inertia that the top of the fluid layer exerts while the wafer below rotates faster and faster. Eventually, the fluid is thin enough to be completely co-rotating with the wafer and any evidence of fluid thickness differences is gone. Ultimately, the wafer reaches its desired speed and the fluid is thin enough that the viscous shear drag exactly balances the rotational accelerations. In our case the rotation speed was 2000 r.p.m for 20sec.

The third step is when the substrate is spinning at a constant rate and fluid viscous forces dominate fluid thinning behaviour. This step is characterized by gradual fluid thinning. Fluid thinning is generally quite uniform, though with solutions containing volatile solvents, it is often possible to see interference colours

"spinning off", and doing so progressively more slowly as the coating thickness is reduced. Edge effects are often seen because the fluid flows uniformly outward, but must form droplets at the edge to be flung off. Thus, depending on the surface tension, viscosity, rotation rate, etc., there may be a small bead of coating thickness difference around the rim of the final wafer.

The fourth stage is when the substrate is spinning at a constant rate and solvent evaporation dominates the coating thinning behaviour. As the prior stage advances, the fluid thickness reaches a point where the viscosity effects yield only rather minor net fluid flow. After spinning is stopped many applications require that heat treatment or "firing" of the coating be performed.

In our case the films were allowed to dry under ambient conditions for 24 hours to ensure total removal of the solvent. When the films were treated by heat unwanted decrease in the concentration of photochromic molecules was observed. All the spin coated films were prepared in clean room conditions.

4
Preliminary results

4.1 Observation of the volume change

The implementation of photochromic polymer systems as actuators in micromachines for inducing photocontrolled movements at sub-micron scale was revealed in previous work. We have already demonstrated that photochromic compounds embedded in polymeric matrices behave as photocontrolled micro/nano actuators [24]. Specifically, polymer films doped with photochromic spiropyran molecules were irradiated with laser irradiation, at 248 nm, and surface displacements due to volume changes of a few hundred nanometers were observed by using double-exposure holographic interferometry in reflection mode. These changes were attributed to mechanical effects arising from stresses developed in the polymeric

matrix due to the UV light-induced conversion of the incorporated spiro molecules to their isomeric merocyanine form. Subsequent irradiation of the photochromic polymer film at 532 nm leaded to the recovery of the volume to its initial condition. The reproducibility of these controlled alterations was investigated by repeating the UV–visible irradiation cycles for several times on each sample.

4.2 Demonstration of photochromic polymer system as photoswitchable cantilever

Subsequent experiments were performed in order to develop photochromic polymer systems in the use of laser controlled molecular actuator [25]. One edge of the photochromic polymer film was mounted onto a stable base. Upon appropriate irradiation with laser pulses, the polymeric cantilevers changed their volume reversibly, since the structural transformation of the incorporated photochromic molecules induced mechanical alterations of the host matrix. The transformations induced in the spiro compound were upon irradiation at 355 nm, converting it to the merocyanine isomer. The reverse effect occurred upon irradiation at 532 nm. The changes in volume of the polymeric cantilever were translated into bending. This bending was detected by monitoring the deflected light of a He–Ne laser by the free edge of the cantilever on a graduated screen.

In figure 4.2.1. the leftward movement of the deflected beam indicates that the layer of the film where the UV irradiation is absorbed is **contracted**. This layer carries along the back surface of the film, which is beyond the optical penetration depth, producing the overall bending of the film.

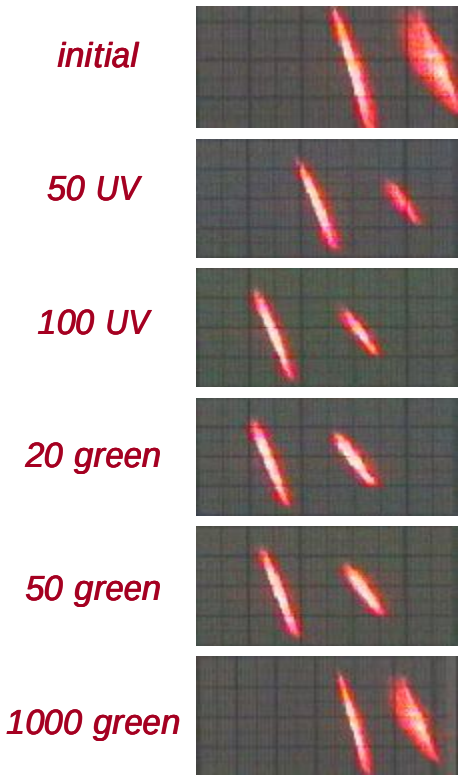

Figure 4.2.1: Monitoring the movement of the deflected beam from the back surface of a 5.0% wt photochromic-doped PEMMA film (150μm) after irradiation of the front surface with successive 355-nm- and 532-nm-wavelength pulses (fluence: 25 mJ cm^{-2} and 60 mJ cm^{-2}, respectively).

The first results showed that the cantilever either was starting to move towards its initial state immediately after the first green pulse, following exposure to UV pulses or, the UV pulses and the initial green pulses induced volume changes in the sample towards the same direction. Only after the first few pulses at 532 nm the sample started to revert to its initial condition. In particular, irradiation with UV pulses at 355 nm with a fluence of 80 mJ cm^{-2} caused the irradiated surface of the film to contract, and thus to produce an overall bending of the film. The deflection of the beam in this case moves towards the left. Contraction continues upon irradiation with the first 20 green pulses at 532 nm with a fluence of 190 mJ cm^{-2}. Only after the termination of the green pulses, contraction stops. By additional green pulses, the cantilever reverts to its initial state, causing the deflected beam to move towards right until its initial position. This experiment was repeated several times, and it was nicely reversible [25].

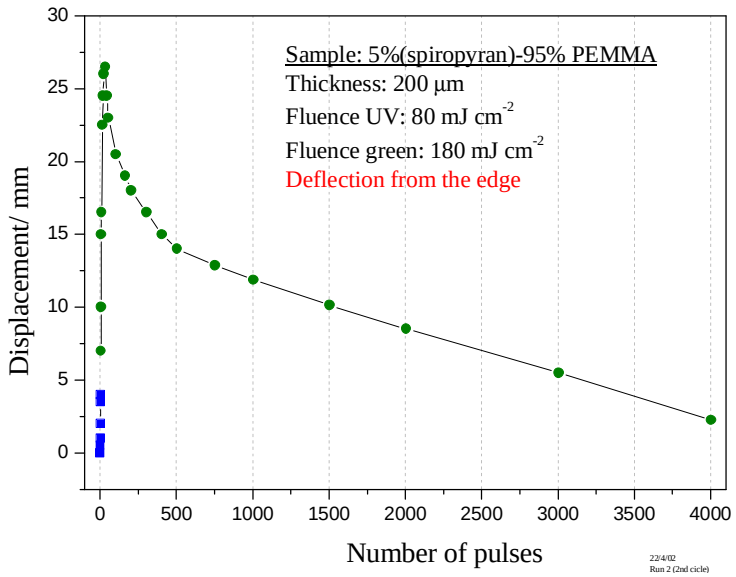

Figure 4.2.2: Displacement of the deflected beam vs. total number of incident pulses.

To this point, two basic mechanisms were proposed for the explanation of the photomechanical changes of the photochromic-doped polymeric matrices, which included spatial disturbance of the matrix. Blair *et al* [26] suggests that the change in volume of the photochromic polymers upon the spiro-to-merocyanine photoconversion may be explained by the closer packing of the polymer molecules upon formation of the planar merocyanine molecules.

On the other hand, Gonzalez-de Los Santos *et al* [27] claims that the fact that spiropyran is nonpolar while merocyanine has a large dipolar moment should have a significant influence on the polymer coil formation and consequently on the volume of the sample.

4.3 Examination of the reproducibility of the photochromic cantilever

The next step was to examine the reproducibility of the above photochromic cantilevers [28]. This was achieved by repeating several irradiation cycles for each sample. In figure 4.3.1 it can be seen that at the first mechanical cycle the sample moves beyond its initial position as it returns, and it relaxes at a “negative” position. This effect may be ascribed to the fact that some stresses are induced into the sample

during the preparation or drying procedure, and they are removed throughout the duration of the first cycle. Indeed, as shown in Figure 4.3.1, this effect occurs only once, during the first optomechanical cycle. In the case of all the following cycles the sample relaxes either before its initial position, or as it reaches it. As the irradiation cycles are increased the cantilever shows a fatigue, which is obvious by the reduction of the overall length of the mechanical cycles, and by the fact that it does not relax every time at its starting position. Nevertheless, despite the fatigue of samples, the optically induced mechanical actuation of the polymeric cantilevers is nicely demonstrated for several repetitions.

In the case of the experiments presented in Fig. 4.3.2 the bending of the polymeric cantilever occurs almost exclusively upon irradiation with green laser pulses. The preceding UV laser pulses induce only an insignificant bending to the cantilever and thus the deflected beam remains almost stable. However, when the samples are irradiated exclusively with green pulses, without any previous UV irradiation, no movement occurs. This observation indicates that the initial UV laser pulses induce the transformation of the spiropyran molecules to some merocyanine stereoisomers (colouration process). This process is essential for any following mechanical transformations of the sample. It cannot though by itself to contribute significantly to the length alterations, and thus to the bending of the cantilever.

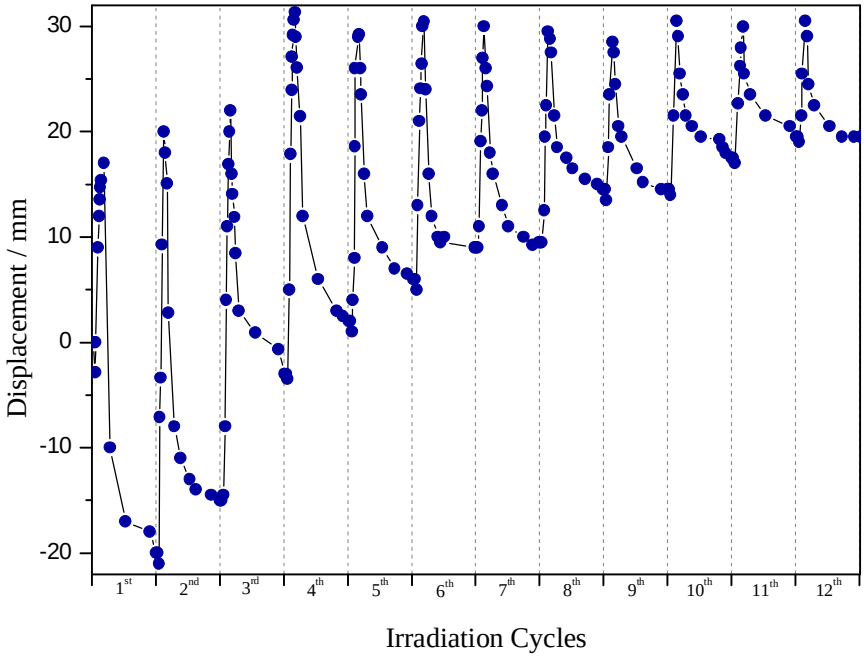

Figure 4.3.1: Successive displacement cycles of a He-Ne beam deflected from the freestanding edge of a photochromic-polymeric cantilever, following the irradiation of the cantilever with successive UV (308 nm) and green (532 nm) laser pulses.

Another remarkable point is that the maximum displacement and thus the maximum volume contraction is obtained at the first optomechanical cycle and it is calculated that it corresponds to about 0.11 % relative contraction. It is obvious from Fig. 3.3.1 that the relative contraction decreases as the mechanical cycles are repeated, due to fatigue of the sample, and after 12 cycles it becomes 0.03 %.

In Figure 4.3.2 is shown that the reversible optomechanical cycle occurs almost exclusively upon irradiation with green laser pulses. The initial ten UV pulses do not induce any significant bending of the cantilever. However, irradiation with exclusively green laser pulses without previous UV pulses induces no movement of the deflected beam. We can therefore conclude that the initial UV pulses are responsible for the transformation of the spiropyran molecules to some merocyanine photoproducts. This photocoloration process is necessary for any further mechanical transformation. However the photocoloration process by itself is not able to induce length alteration and therefore any bending of the cantilever.

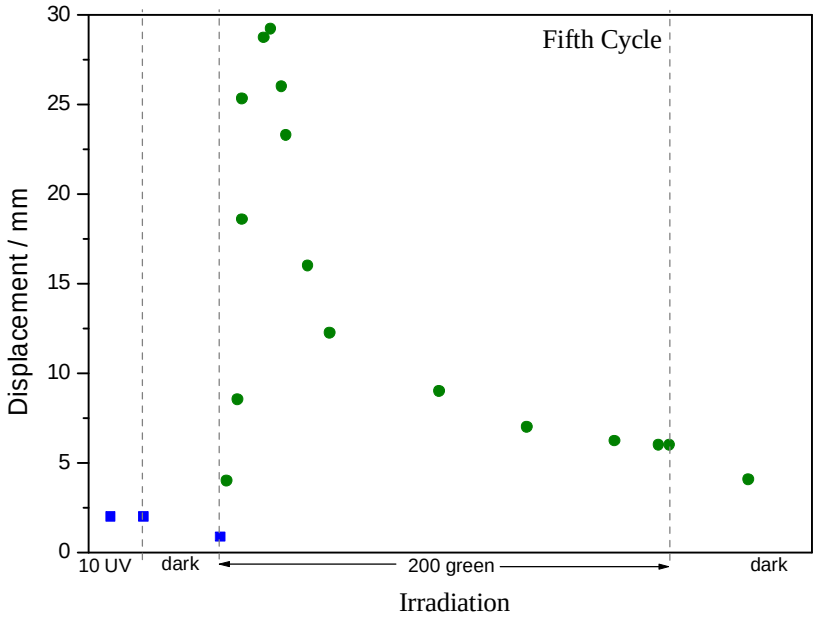

Figure 4.3.2: The fifth displacement cycle of a He-Ne beam deflected from the freestanding edge of a photochromic-polymeric cantilever.

The observed contraction of the samples can be ascribed to the interconversion of the different merocyanine molecules upon light absorption. Indeed, as mentioned by Görner, eight merocyanine stereoisomers, with respect to the three partial double bonds, exist (the *cis* isomers: TCT, TCC, CCT, CCC, and the *trans* isomers: TTT, TTC, CTC, CTT [29]. It is reported many times in the literature that the photoprocesses in the related merocyanines involve several stereoisomers, which convert to the most stable form(s) [29,15]. The stable form(s) depends each time on the host medium. In the present experiment, the energy of 2.3 eV given to the merocyanine isomers by irradiation at 532 nm is enough to exceed the activation barrier height for their conversion back to the spiropyran form, but also to convert them to the other merocyanine stereoisomer(s) [15].

Therefore we can conclude that the mainly responsible procedure for the contraction of the cantilevers is the absorption of visible light from the merocyanine isomers, previously formed upon UV irradiation, and their subsequent conversion to other stable merocyanine isomers. The contraction of the samples upon UV laser light irradiation, when higher UV fluences are used, can be ascribed to the fact that merocyanine isomers absorb in the UV region as well. The pathways that lead to the stable isomer(s), may also play an important role i.e. the short-lived merocyanine isomers (the cis, as so called, isomers).

We may easily observe that in figure 4.2.2 the number of green laser pulses needed for the recovery of the sample to the initial position, or close to it, is about an order of magnitude greater (1500-4000). However, in the experiments presented in figure. 4.3.2, 200 green pulses are more or less capable of returning the sample in its almost initial position. In the experiments presented in fig 4.2.2 we were leaving the cantilevers to relax for 10 seconds each time, after their irradiation with few laser pulses (1-10). Therefore, every time that we were capturing the image of the deflected beam, the cantilever was relaxed. In the other hand, in figure 4.3.2 the monitoring of the deflection occurs simultaneously with the irradiation of the samples, which is continuous until the final relaxation of the samples. The optically induced mechanical effects differ to some extent in these two cases. The different optical actuation may be due to the fact that in the first case the short-lived, non-stable isomers are converted after each irradiation step to the stable ones, while in the second case, they are possibly continuously interconverted until their final return to the closed spiropyran form.

4.4 Fluorescence emission of the stable photoproducts from the photochromic-polymer samples

To elucidate the pathways of the transformations of the photochromic dopants during the photoinduced mechanical cycles, fluorescence emission experiments were performed with the same parameters of the laser pulses as in the case of the optomechanical experiment for correlation reasons. Figure 4.4.1 shows the fluorescence emission of the merocyanine isomers, formed during one irradiation cycle of a film 5.0% by wt 6-NO_2-BIPS in PEMMA. The sample is irradiated with 10 UV pulses (308 nm) of ~50 mJ cm^{-2}, followed by green pulses (540 nm) of ~110 mJ cm^{-2}. The repetition rates of the excimer laser and of the Nd:YAG laser are 2 Hz and 10 Hz respectively. The thickness of film is 7.0 μm and is optically thin, as fluorescent type experiments require. Therefore, the fluorescence intensity can be considered to be exactly proportional to the merocyanine isomers formed in the sample, without the need for “inner-filter” effect corrections (self-absorption).

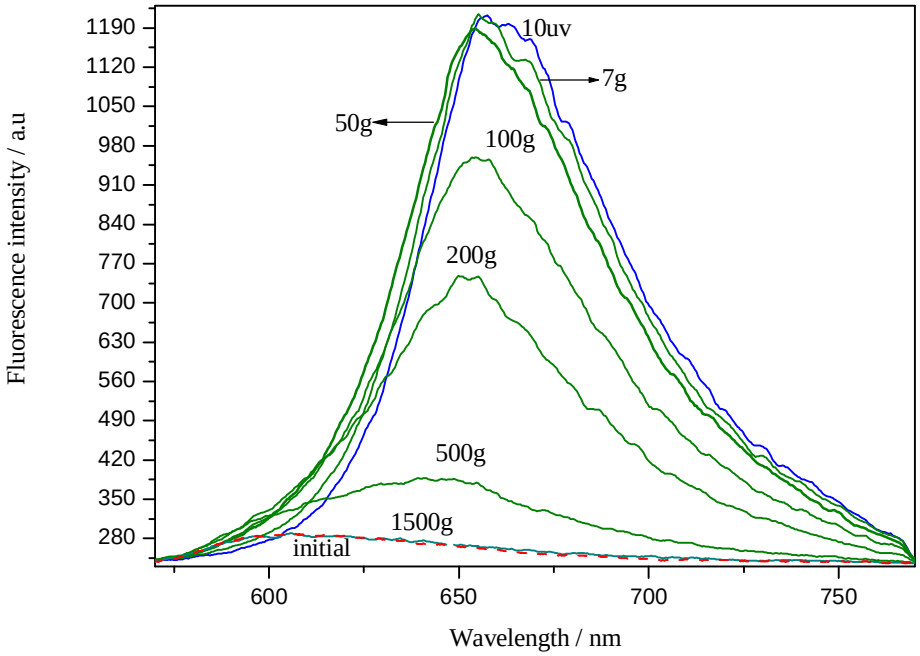

Figure 4.4.1: Fluorescence spectra from 5.0% by wt 6-NO_2-BIPS in PEMMA films after irradiation with subsequent UV (308 nm) and green (540 nm) laser pulses.

Initially, the sample does not fluoresce, since the incorporated in the polymer matrix molecules are the non-fluorescing spiropyrans [7]. The UV laser pulses convert the spiropyran molecules to their merocyanine isomers. The formed isomers after irradiation with 10 UV pulses show a characteristic fluorescence spectrum, which is shown in figure 4.4.1. The green laser pulses, which follow the UV pulses, are responsible for the conversion of the already formed merocyanine molecules, to other merocyanine stereoisomers, with different structures, and thus, different fluorescence spectra. This conversion is demonstrated in figure 4.4.1 as the fluorescence spectra change, and their maxima move towards smaller wavelengths upon irradiation with the first green laser pulses. After additional irradiation of the sample with >30-50 green laser pulses the fluorescence spectra not only move even further towards smaller wavelengths, but also their intensity decreases. This decrease indicates, that the open form merocyanine molecules return gradually to the closed, non-fluorescing, form. It can be seen that after 1500 green pulses the fluorescence spectrum has return completely, and therefore it can be concluded that all the molecules, incorporated in the polymer, are converted to the spiropyran form.

The probe beam that induces the fluorescence emission shown above irradiates the sample one minute after the end of the pump beam, to ensure that all the photochemical procedures in the samples are completed, and thus, the molecules that fluoresce are the finally formed stable merocyanine isomers.

4.5 Time-resolved fluorescence experiments

To elucidate the pathways of the stereoisomeric transformations into the polymer matrix we performed time-resolved fluorescence experiments [45]. Therefore we monitored the short-lived merocyanine (MC) isomers formed into the pump pulses or in short time periods after them. These experiments led to the clarification of the role of the stereoisomeric transformations to the optomechanical cycles of the photochromic cantilever. Figure 4.5.1 a shows the characteristic fluorescence spectra from metastable MC photoproducts at later stages of the photomechanical cycle. Distinct bands appear at longer wavelengths (> 680 nm) than those corresponding to the stable MC stereoisomers. Such bands have been previously recorded in transient fluorescence measurements and attributed to aggregates (dimers or complexes of higher stoichiometry) of the MC molecules [30-32]. These aggregates are the result of dipole-dipole interactions between the MC stereoisomers due to their zwitterionic character. Lenoble *et al* [18] proposed that the MC aggregates of the 6-NO_2-BIPS in solvents are produced by a bimolecular reaction between the triplet state of a *cis* metastable and a *trans* stable MC stereoisomer as mentioned in the theoretical session. Li *et al* [33] have added that the aggregate observed by Lenoble is not stable but it decays within μs. The formation of this type of aggregates is in agreement with the existence of intermediate photoproducts in our experiments.

The initial increasing formation of the aggregates (Figure 4.5.1 b) is in correspondence with the increasing volume contraction of the films caused by the first green pulses. Moreover, the subsequent decrease of the aggregates can be correlated to the beginning of the volume recovery, and their disappearance with the eventual restoration of the sample. After the disappearance of the MC aggregates, the remaining MC isomers continue to fluoresce at shorter wavelengths even after irradiation by more than 200 green pulses. This explains why the film returns to its initial position although its colour is not fully recovered.

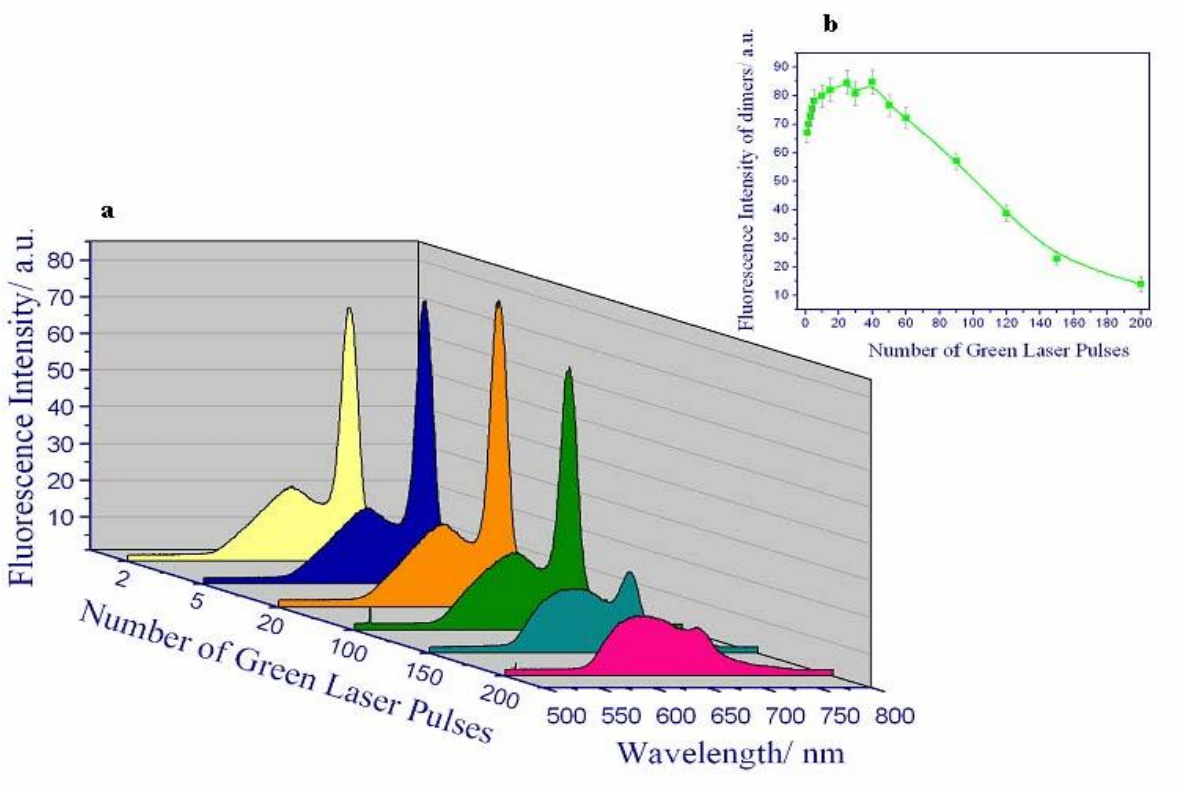

Figure 4.5.1: a) Fluorescence emission spectra of the intermediate/metastable fluorescing photoproducts recorded during each green laser pulse (532 nm, 70 mJ cm^{-2}). The emission band at the wavelengths 680-720 nm is attributed to the aggregates of the MC molecules. b) Maximum emission intensity of the aggregates vs. number of green pulses.

In our system, short scale motion of the polymer chains may occur in order to reduce the density fluctuations attributed to the reduction of effective partial molar volume of the MC stereoisomers, due to aggregates formation. The reduction of the MC partial molar volume results into an increase of the effective free volume in the polymer matrix, giving rise to a decrease of its effective T_g. A reduced T_g together with the temperature rise during the laser pulse favour a decrease in the viscosity of the sample. This allows an enhancement of the motion of the polymer chains, which causes the macroscopic contraction. Next, the formation of the aggregates decreases until it stops due the return of the MC molecules to the initial SP form, and the sample recovers to its initial volume, since the polymer chains are forced to return to their initial positions. The above described processes differ from those presented in previous works, in which the photoisomers either induce structural changes in the attached macromolecules, or move with them the macromolecular chain on which they are attached to induce photomechanical changes [34-37]. The mechanical

changes due to such processes are slow (tens of seconds to hours) in contrast to the fast cycle observed here. Further optimisation of the laser parameters involved (pulse duration, fluence, repetition rate) may lead to an even faster response.

5

Absorption measurement results

5.1 Study of the degradation process

Photochromism is a nondestructive process, but side reactions may occur. The loss of performance over time, due to chemical degradation of a material, is termed “fatigue”. Usually, the major cause of damage of photochromic substances is oxidation. Some spiropyran applications (photolithographic plates, fluid flow visualization) are not significant limited by the fatigue. Commercial applications though without fatigue limitations are mandatory. The use of macromolecules as matrices with spiropyrans results to the fact that the polymer modifies the properties of the spiropyran and the behavior of the spiropyran gives information about the polymer. Hence, polymer control of the photochromic properties may significantly lower the rate of fatigue, probably by sterically hindering the approach of oxygen to the dye moiety.

As previous reported and marked the effect of the volume change in the photochromic cantilevers is reduced with the resumption of the irradiation cycles. In previous chapter it was analytically demonstrated that a maximum displacement of the deflected beam and thus a maximum volume contraction of the sample was

observed in the first optomechanical cycle and corresponded to about 0.11 % relative contraction. The relative contraction decreased with the repetition of the optomechanical cycles, due to fatigue of the sample, and after 12 cycles it became 0.03 %.

A series of absorption measurement experiments were performed in order to study and furthermore to avoid the observed fatigue process. The possible mechanisms for the presence of fatigue in the photochromic films may be attributed to three basic phenomena. The first deals with the presence of oxygen to the atmosphere were the experiments are performed and thus oxidation reactions may take place. Another possible reaction of the energy that the samples absorb by the lasers can be related to bonding formation of the photochromic molecules with the polymer matrix. Different chemical or physical effects related to evaporation of the photochromic molecules or bond leakages cannot be excluded from the possible fatigue responsible mechanism.

For elucidating the above responsible for the fatigue process mechanisms, absorption experiments were performed using different polymer matrices, under the same irradiation conditions to clarify the role of the macromolecule chain and the way the photochromic molecule interacts with the different each time polymer matrix, as well as different UV wavelengths to examine the influence of the laser wavelength. The matrices that were examined have different chemical (monomer chain, molecular weight) as well as physical (glass transition temperature, elastic modulus, e.t.c) properties and are presented in the following table.

	Monomer	T_g	M_w	M_w/M_n
Polystyrene (PS) ***(Polymer Source)***	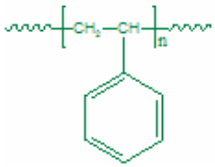	~100°C	44000	1.06
Poly(methyl methacrylate) (PMMA) ***(Polymer source)***	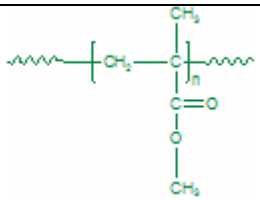	95 -106°C	112300	1.09
Poly(ethyl methacrylate-*co*-methyl acrylate) (PEMMA) ***(Aldrich)***	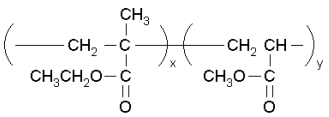	48°C	~100,000	

Table 5.1.1: Chemical types and physicochemical properties of the polymers used.

The photochromic molecule used was the 1',3'-dihydro-1',3',3'-trimethyl-6-nitrospiro [2H-1-benzopyran-2,2'-(2H)-indole] with a stable concentration of 10% w.t in the different polymer matrices. All the samples were prepared in dichloromethane solutions under clean room conditions in a customary manner. They were spin coated on quartz substrates at 2000 r.p.m for 20 sec. These conditions ensure a uniform surface roughness of the film as well as a homogenous film concentration. A KrF laser operating at λ_{laser}=248 nm, $\tau_{pulse}\approx$ 15 ns (TUI Laser, BraggStar 200) and an Nd:YAG laser operating at λ_{laser} = 532 nm, $\tau_{pulse}\approx$ 15 ns (Spectron Laser Systems), were used for pumping the sample.

The experimental results presented below show 10 irradiation cycles. The sample that we examined was a polymeric film consisting of 10%SP in 90% PEMMA. At figure 5.1.1 a), each cycle consists of 10 UV laser pulses at 248nm followed by 1000 additional green laser pulses for the recovery of the photochromic compound to its initial state.

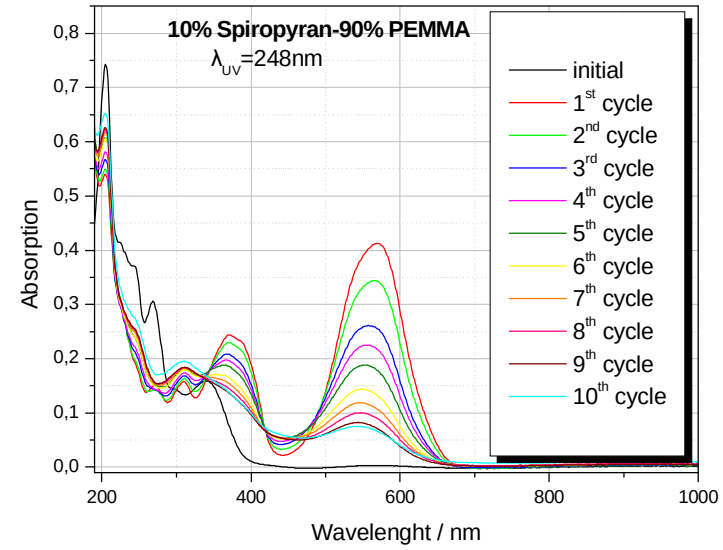

a)

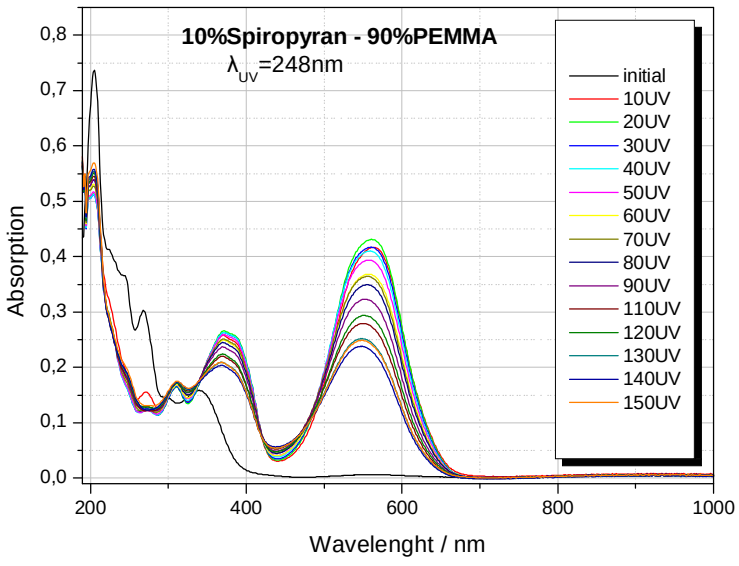

b)

Figure 5.1.1: Absorption spectra of 10%Sp-90% PEMMA at 248nm. UV cycles followed by green pulses for the recovery of the film (a). Subsequent UV irradiation of the photochromic substrate (b).

On the contrary, in the figure 5.1.1 b) only UV pulses were used to irradiate the same photochromic film in different spot area. Each time the absorption spectrum was collected after 10 additional UV pulses until we reached 150 pulses. Both fluences of the lasers remained constant and equal to 25mJ/cm^2 for the UV laser and 65mJ/cm^2 for the green laser respectively. It is obvious that the green laser pulses used for the return of the sample in the left case affect significant the influence of the fatigue. The absorbance after 100 UV pulses is greater in the case where the sample is not each time returned to its initial state by a factor of 4,6. By

the fact that the fatigue process takes place with much less UV pulses when green pulses are used for the recovery, we may rightly conclude that bond breaking procedure is not the cause of the fatigue existence since in both cases (*(a)* and *(b)*) the number of the UV pulses needed to break chemical bonds would be the same given that the energy of the visible laser is not significant for bond cleavage.

This result is highly verified by the repetition of the experiments and by the fact that the use of different polymer matrix as well as different UV laser wavelength gives the same factor for the fatigue rate. More specifically, by performing absorption measurements in samples consisting of 90% polystyrene doped with 10% spiropyran molecules pumped with a 308-nanometer laser we calculated the exponential decays in two occasions. In the first one the sample was irradiated with UV pulses followed by 1000 green pulses for the return each time to its initial position. In the second case we irradiated the sample with subsequent UV pulses collecting the absorption spectrum after a certain each time number of pulses. The fluence of the UV laser was 50mJ/cm^2 while the green laser operated at fluence of 65mJ/cm^2. The results are shown in the following figure.

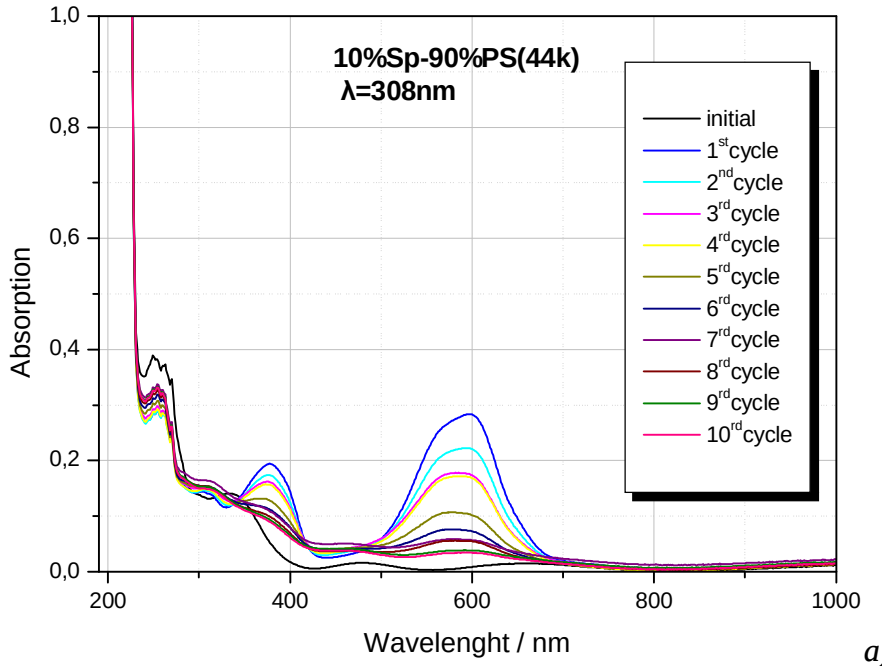

a)

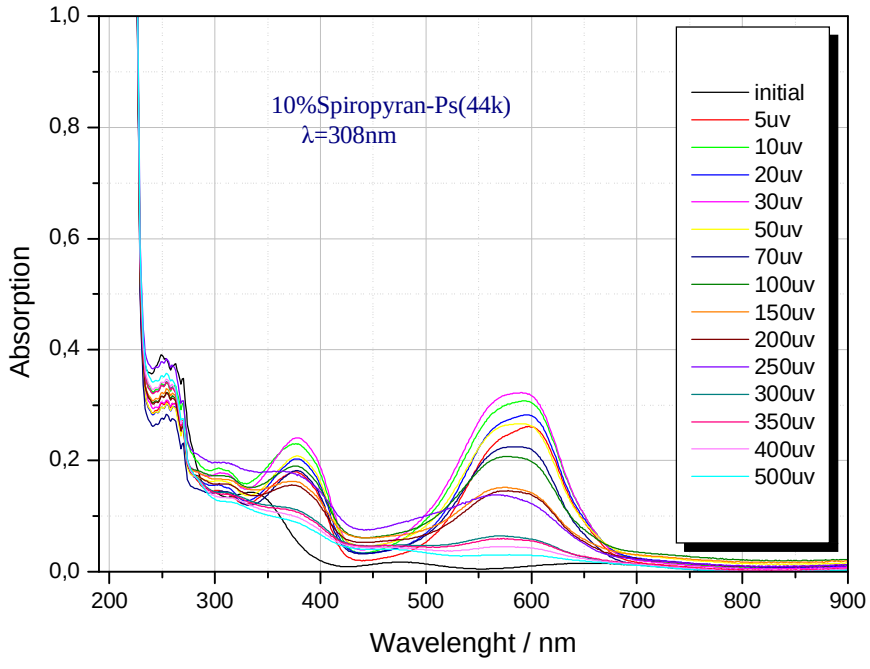

Figure 5.1.2: Absorption spectra of 10%Sp-90% PS (a) *and 10%Sp-90%PS* (b) *at 308nm*

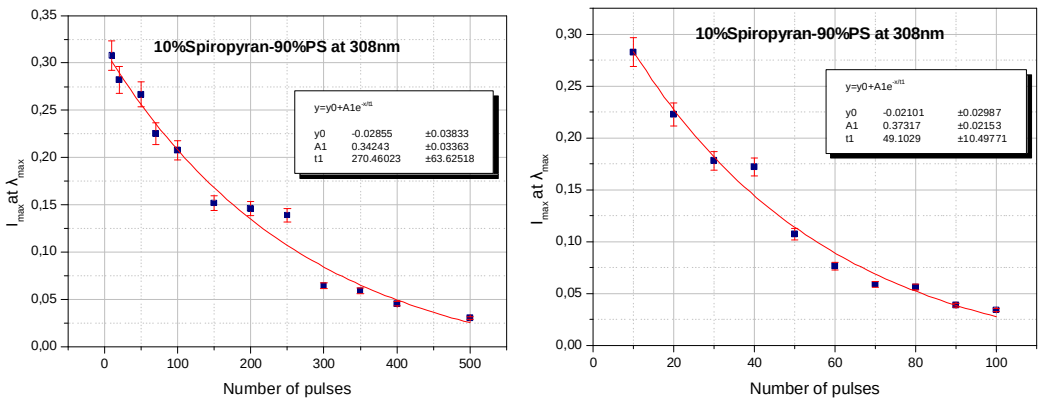

Figure 5.1.3: Exponential decays of the absorption intensity on the samples 10%Sp-90% PEMMA and 10%Sp-90%PS

Taking into account the points were the absorption intensity is reduced to half of its initial value and calculating the slopes we conclude that the decay in the case where green pulses have been used for the back conversion of the sample is larger by a factor of 4,9 as in the case of PEMMA used as a polymer matrix. Thus the previous results in which no bond cleavages occur during the irradiation procedures are efficiently verified.

In order to examine the role of the polymer matrix we performed identical absorption measurements for a sample of 10%SP in 90%PEMMA and 10% of the same Spiropyran photochromic molecule in 90% PS, using a KrF laser operating at λ_{laser}=248 nm for the conversion of the Spiropyran molecules to the Merocyanine compounds.

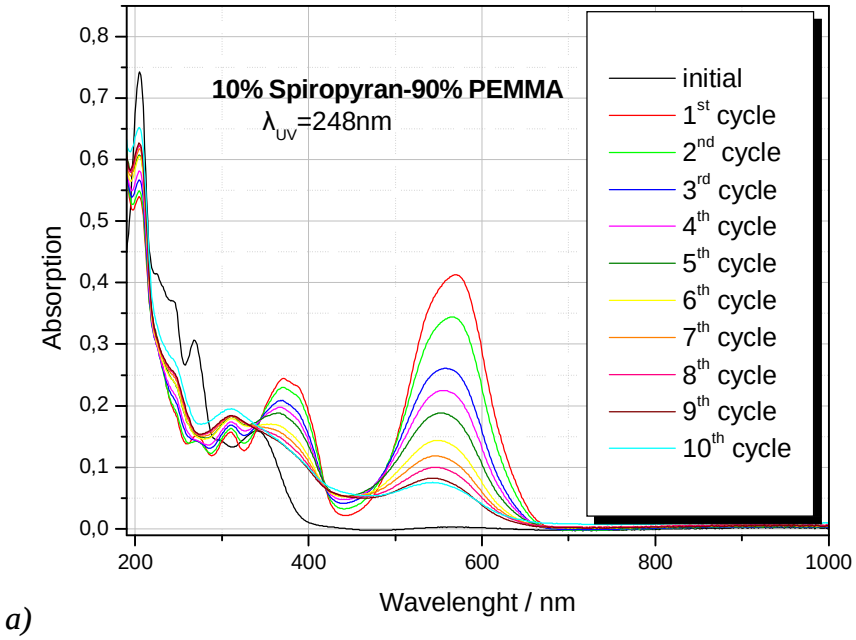

a)

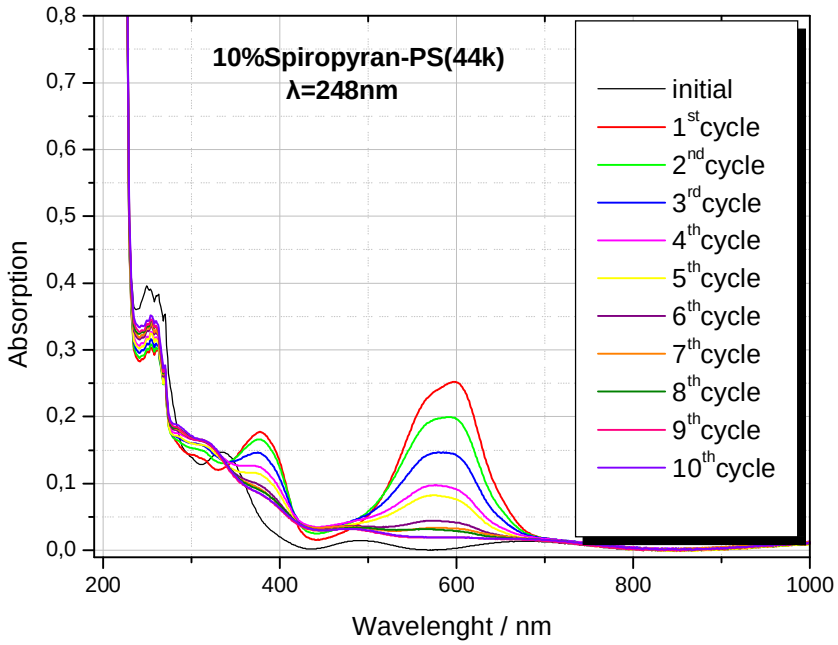

b)

Figure 5.1.4: Absorption spectra of 10%Sp-90% PEMMA (a) and 10%Sp-90%PS (b) at 248nm

In figure 5.1.5 the maximum absorbance corresponding to the maximum wavelength of the peak appearing in the visible region is plotted versus the number of the UV pulses. A first order exponential fit indicates a larger decay in the case when polystyrene is used as a polymer matrix. Taking into account only the first three points in which the absorption has been reduced to the half of its initial value we may rightly assume a linear approach to these three marks. By calculating the slopes of the two linear fits we found out that when polystyrene is mixed with the photochromic molecules the exponential decay of the absorption is reduced by a factor of ~1,5.

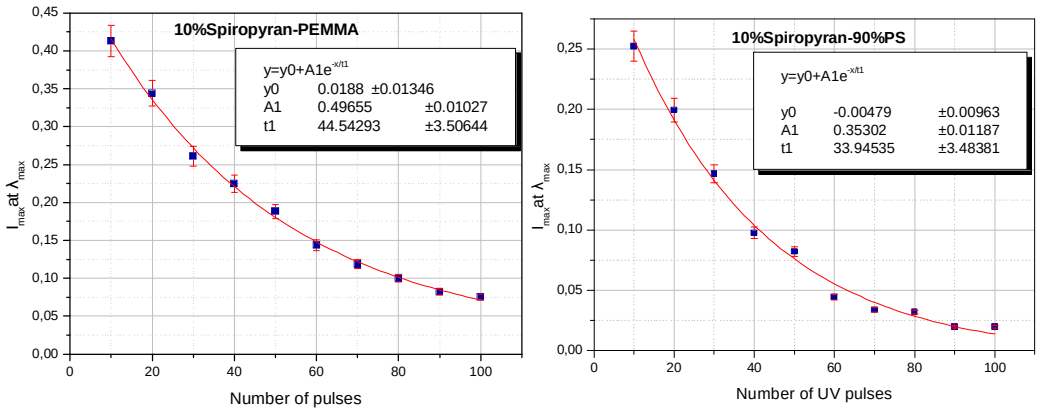

Figure 5.1.5: Exponential decays of the absorption intensity on the samples 10%Sp-90% PEMMA and 10%Sp-90%PS

It is crucial to mention here that polystyrene macromolecule attends a significant absorption in the UV region since benzene rings are present in its chemical form. Thus we expected a lower decay of the fatigue process in the case were PS is used, as a macromolecular chain since less photons would be left for the photochromic molecules to absorb. The fact that the opposite phenomenon was observed can be attributed to the fact that polystyrene is more likely to oxidise under atmosphere conditions since it absorbs remarkably strong in the UV region in respect to the other polymers used in the present experiments. Typically, the oxidation of organic materials occurs through the production of a variety of radical species. The formation of radical species can be tracked and used as an indicator of polymer degradation.

Subsequently, the factor of the wavelength influence was studied. Similar experiments were performed using a KrF laser operating at λ_{laser}=248 nm and a XeCl laser operating at 308 nm, $\tau_{pulse}\approx$ 30 ns (Lambda Physik, EMG 201 MSC) for

the conversion of the Spiropyran molecules to the Merocyanine for a 10%SP-90%PS film.

Varying the number of incident photons per pulse that the photochromic molecules absorb would influence the fatigue of the Spiropyran samples. With a subsequent absorption of the polymer matrix less photons would be left for the photochromic compound to absorb. Therefore in order to compare the wavelength influence to the fatigue process the factor of the number of photons available to the Spiropyran molecules should be excluded. The absorption intensity of the polystyrene at 248nm is double comparing with the intensity at 308nm. Thus in order to perform correct measurement the fluence of the UV laser was 25mJ/cm^2 in the case of 248nm and 50mJ/cm^2 in the case of 308nm.

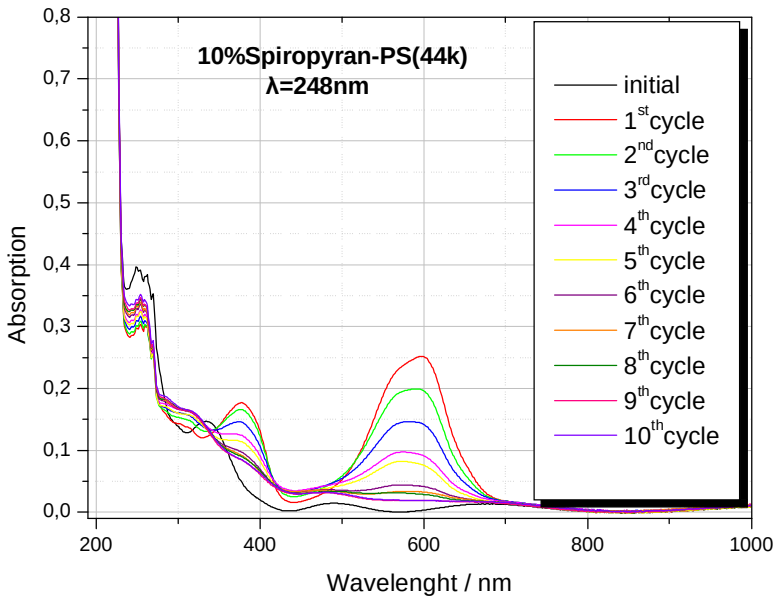

a)

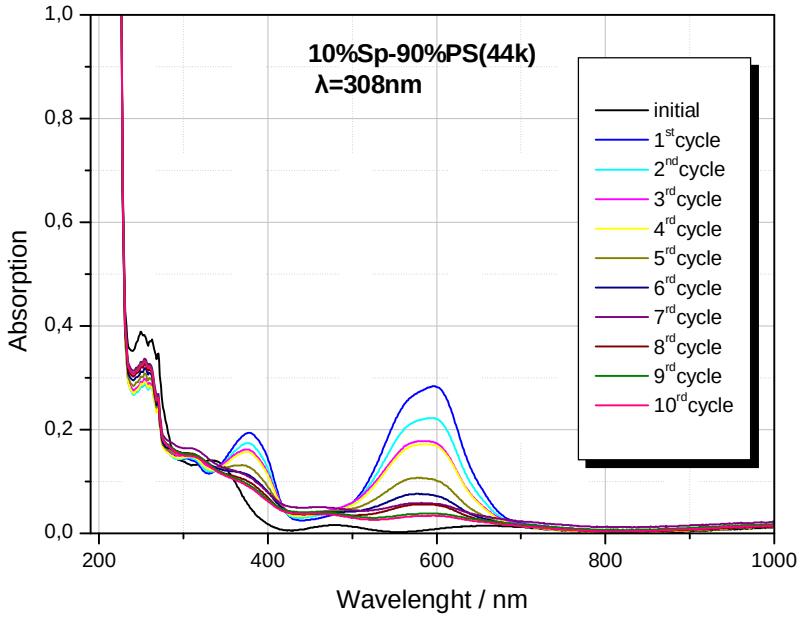

b)

Figure 5.1.6: Absorption spectra of 10%Sp-90% PS (left) *and 10%Sp-90%PS* (right) *at 248nmand 308nm respectively*

By employing the following results of the exponential decays for the absorption intensity versus the number of pulses as previous, we conclude that the wavelength does not influence the fatigue process when no additional absorption procedures take place. The decays for the two cases of 308nm and 248nm irradiation were found with minor differentiations.

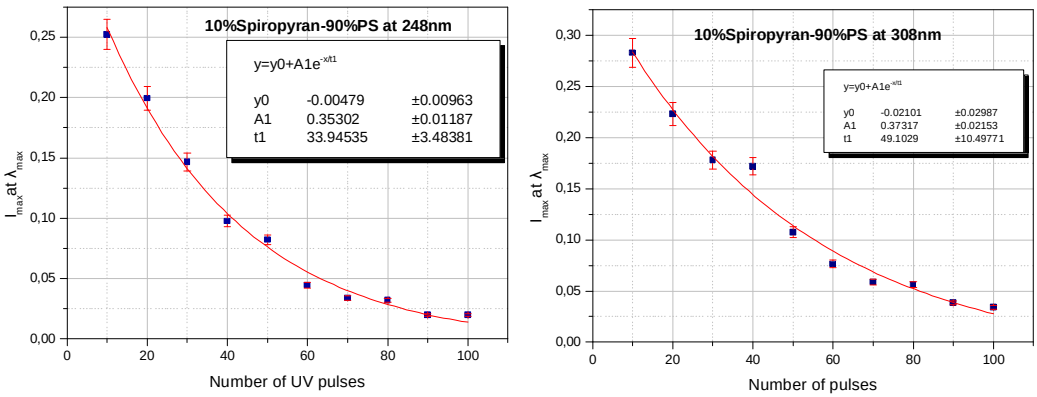

Figure 5.1.7: Exponential decays of the absorption intensity on the samples 10%Sp-90% PS at 248nm and 308nm respectively

Conclusively we may assume that the fatigue process that occurs in the photochromic polymer samples is certainly not attributed to bond cleavages of the

incorporated molecules. To exclude though the bond formation between the photochromic molecule and the polymer matrix FTIR experiments are essential. No significant evidence though for the existence of bond formation was observed. Performing absorption measurements using different polymer matrices and wavelength of the UV laser we may significantly suppose that the fatigue process is almost exclusively attributed to photooxidation. In the case where polystyrene is used as a matrix a more intense contribution of oxidation takes place. No influence of the UV laser wavelength was observed. Thus performing the experiments in nitrogen environment would provide further evidence for the role of photooxidation. This is discussed in chapter 5.2.

5.2 Optimization of the photochromic polymer systems

The rusting of metals, the process involved in photography, the way living systems produce and utilize energy, and the operation of a car battery, are but a few examples of a very common and important type of chemical reaction. These chemical changes are all classified as "electron-transfer" or oxidation-reduction reactions. The term, oxidation, was derived from the observation that almost all elements reacted with oxygen to form compounds called, oxides. The process of oxidation cannot occur without a corresponding reduction reaction. Oxidation must always be "coupled" with reduction, and the electrons that are "lost" by one substance must always be "gained" by another as matter (such as electrons) cannot be destroyed or created. Hence, the terms “lost or gained” simply mean that the electrons are being transferred from one particle to another. Photooxidation can simply be determined as an oxidation reaction induced by light. Nitrogen is a non-reactive gas, which finds several applications in the chemical industry. It is used to dilute reagent gases, to increase the yield of some reactions, to decrease the fire or explosion risk of some other reactions and as far as we are concerned, to avoid the oxidation.

The phenomenon of UV oxidation may play a significant role to the cause of the fatigue observed in our samples. For this reason several absorption experiments were performed to elucidate the effect of photooxidation in the photochromic

films. To this purpose a series of spectrums was collected by irradiating the samples under the presence of atmospheric molecular oxygen. In comparison, exactly the same samples were irradiated under identical irradiation conditions however this time nitrogen in the gas phase was flowing parallel to the samples during the irradiation procedure aiming to remove a significant amount of the molecular oxygen existing in the atmosphere and thus to accomplish a better fatigue resistant performance of the photochromic polymer systems.

A UV-Vis spectrophotometer was used to collect all the absorption spectrums presented below. After the initial spectrum UV pulses operating at 248nm irradiated the sample in succession. The absorption spectrum was collected its time after the end of a certain number of pulses. The increase in absorption near 550 nm is attributed to the formation of the colored form of merocyanine as previous reported. The laser fluence was kept constant and equal to 25mJ/cm^2. Different polymer matrices were also used for determining the effect of photooxidation in the macromolecules combined with Spiropyran molecules.

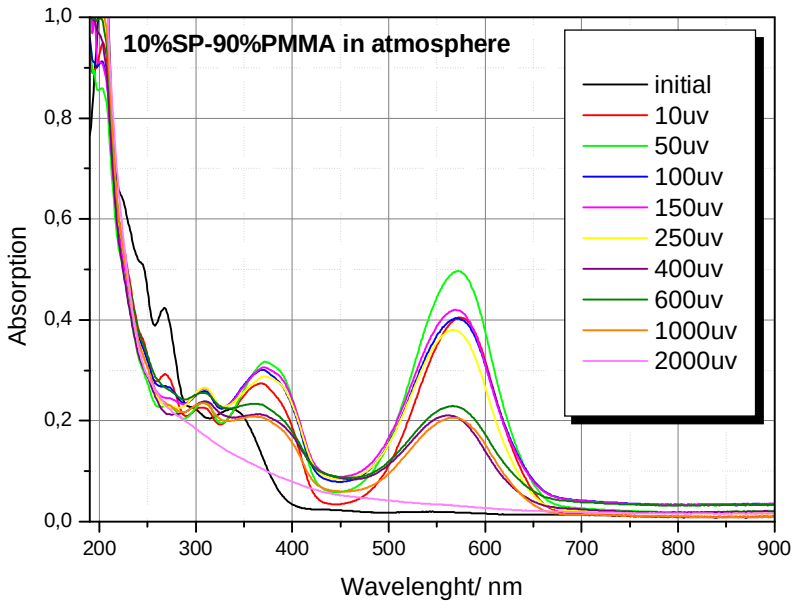

a)

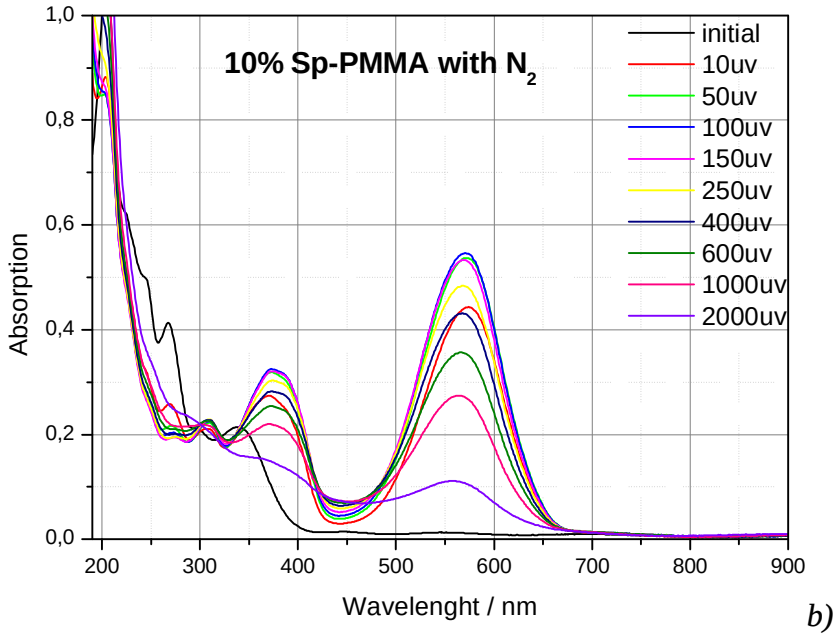

b)

Figure 5.2.1: Absorption spectrum of 10%Spiropyran –90%PMMA with subsequent UV pulses in ambient conditions (a) and with the presence of nitrogen (b).

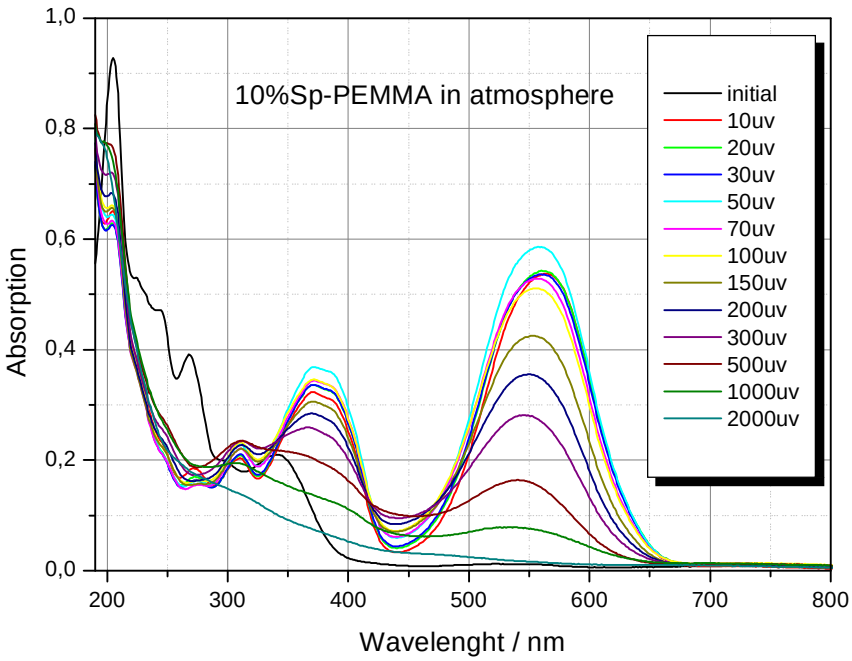

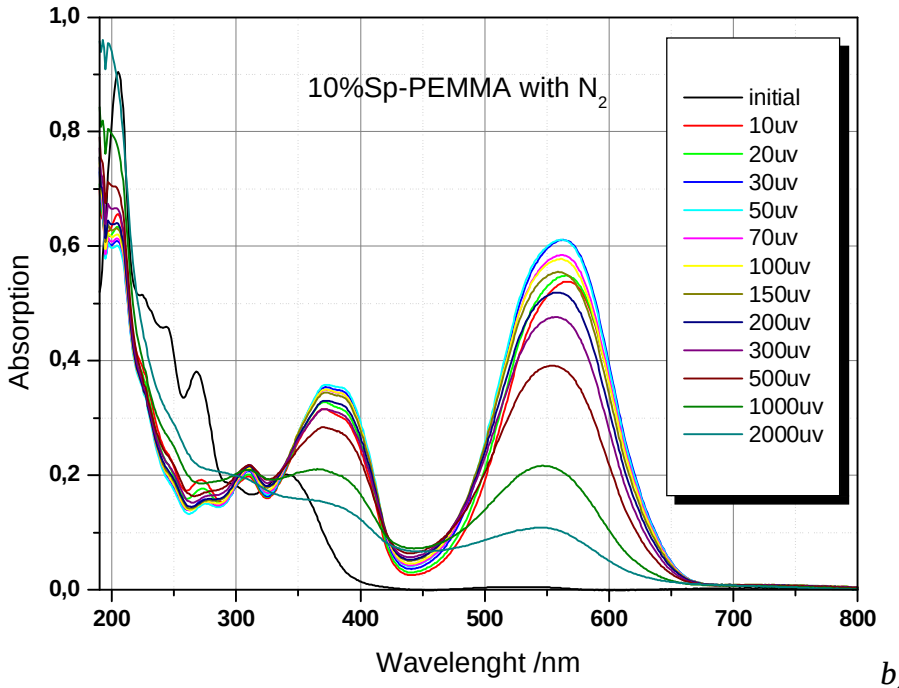

b)

Figure 5.2.2: Absorption spectrum of 10%Spiropyran –90%PEMMA with subsequent UV pulses in ambient conditions (a) and with the presence of nitrogen (b).

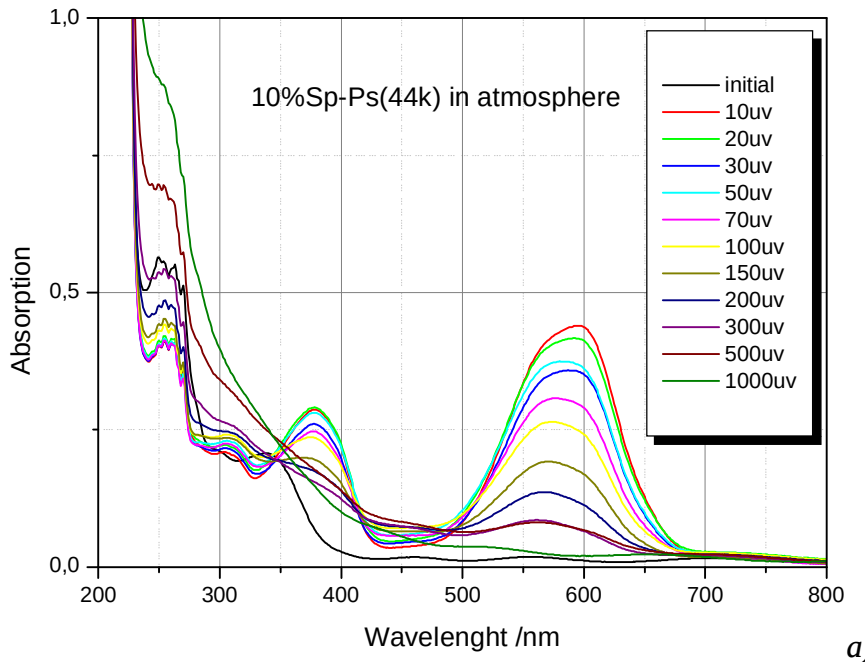

a)

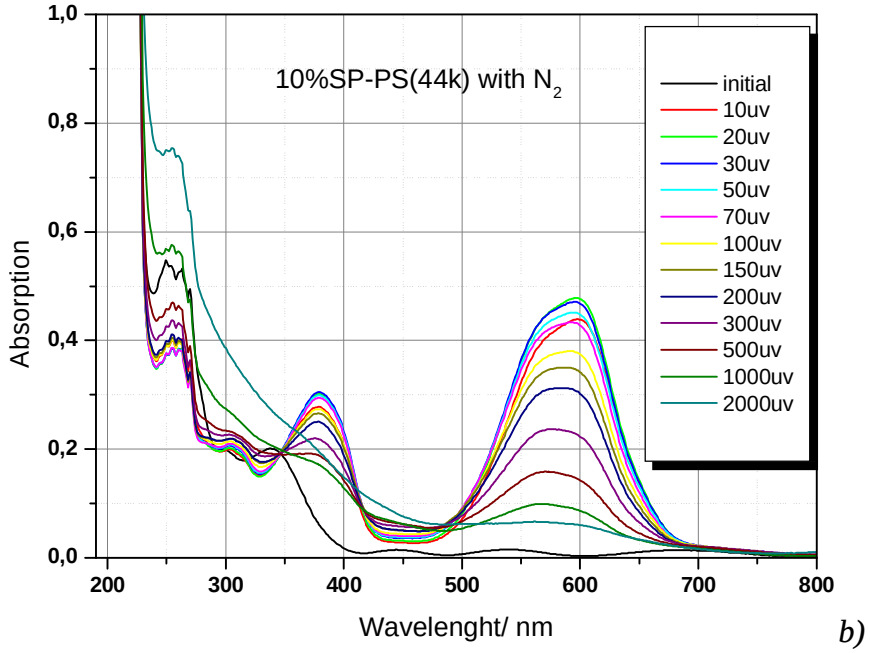

Figure 5.2.3: Absorption spectrum of 10%Spiropyran –90%PS with subsequent UV pulses in ambient conditions (a) and with the presence of nitrogen (b).

For determining the use of nitrogen in optimizing the fatigue resistance, the slope of the absorption intensity decay was calculated in contrast with the slope observed when experiments performed in ambient conditions. For the sample of 10%Spiropyran in 90%PS the fatigue due to oxidation is optimized by a factor of ~1,8 while in the case of 10%Sp-90%PMMA fatigue is reduced 1,9 times and finally when PEMMA is used as a polymer matrix the optimization factor becomes 2,3. Besides the small alterations in the preceding factors no assumption of a greater fatigue resistant owing to the polymer matrix can be made.

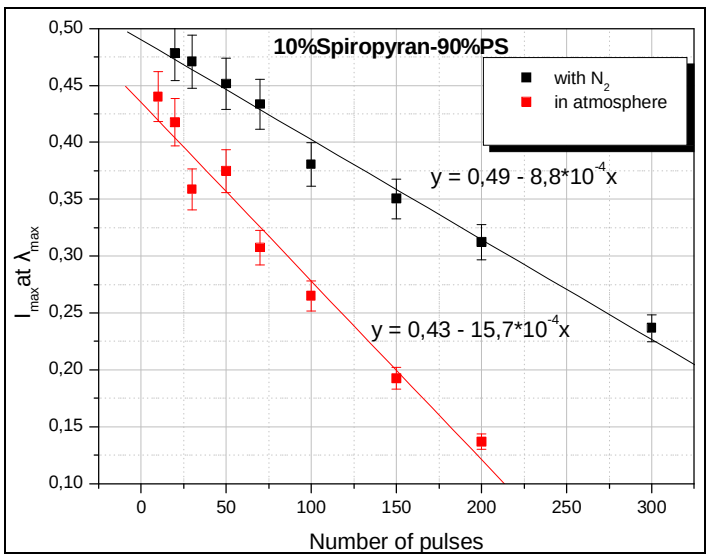

Figure 5.2.4: Maximum absorption intensity versus number of UV pulses in ambient conditions (red plot) and with the presence of nitrogen (black plot).

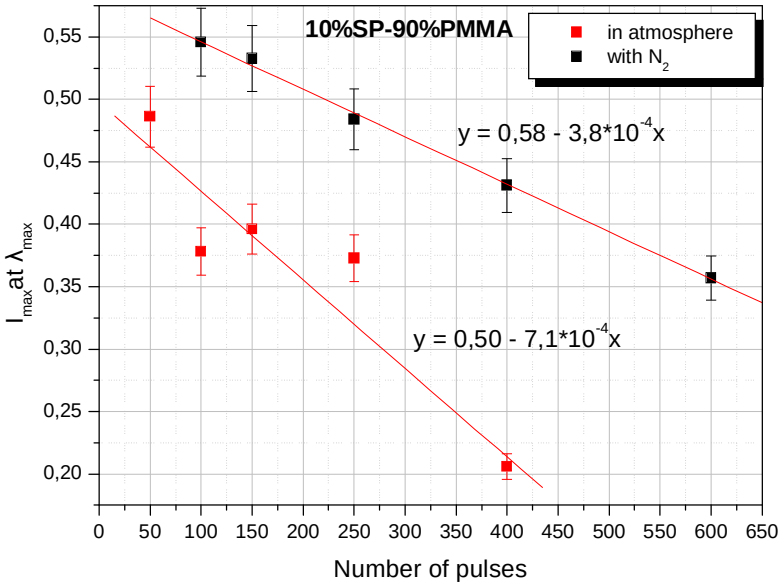

Figure 5.2.5: Maximum absorption intensity versus number of UV pulses in ambient conditions (red plot) and with the presence of nitrogen (black plot) for 10%SP-90%PMMA.

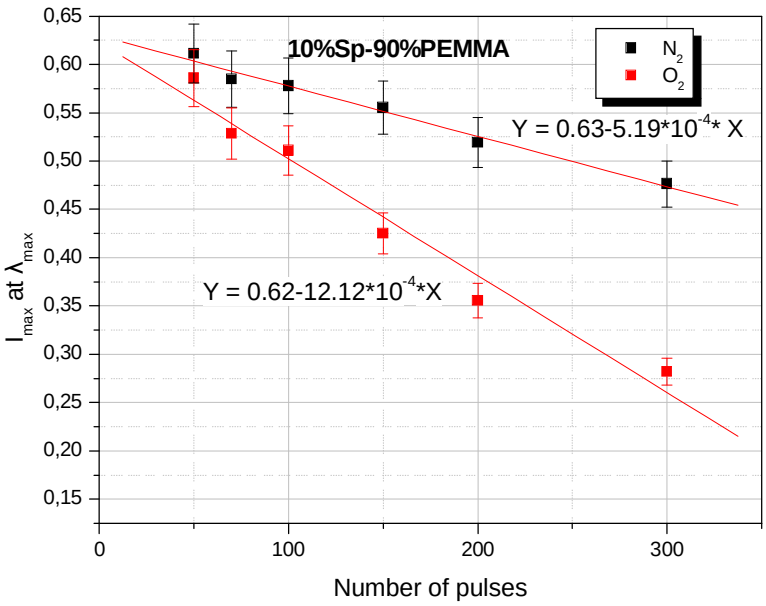

Figure 5.2.6: Maximum absorption intensity versus number of UV pulses in ambient conditions (red plot) and with the presence of nitrogen (black plot) for 10%SP-90%PEMMA.

A great aspect to the achievement of a better fatigue resistance by just flowing gas nitrogen into the samples is the use of chambers full of nitrogen gas to ensure a total removal of molecular oxygen from the samples environment. This would provide a minimized slope decrease limited only by the photobleaching that is the "death" of fluorescence after some excitation-emission cycles, of the Spiropyran molecules. Furthermore preparation of the samples in an environment lacking of oxygen would result in deoxygenated films.

In the above figures we may clearly observe a more abrupt decay of the fatigues slope in the case of polystyrene macromolecule. Having determine the relative slope coefficients of the linear fits of all cases we may safely assume that when polystyrene is used as a polymer matrix a doubled by magnitude decay of the visible absorption peak occurs. This effect has been reported in previous chapter where the fatigue process was studied and is being crosschecked by the above results. It is attributed to the more intense absorption of UV light from polystyrene compared to the absorption of PMMA and PEMMA macromolecules.

6

Study of the switching time of the system

The magnitude as well as the response time of the volume change in the photochromic cantilever is well defined and controlled by the parameters of the lasers used for the manipulation of the volume change and thus for the switching performance. Investigation was performed first to examine the control of the mechanical actuation by altering the parameters of the incident laser pulses and secondly to altering these parameters for faster response time of the systems.

6.1 Experimental procedure

For the macroscopic mechanical actuation of the films a KrF laser operating at λ_{laser}=248 nm, $\tau_{pulse}\approx$ 15 ns (TUI Laser, BraggStar 200) and an Nd:YAG laser operating at λ_{laser} = 532 nm, $\tau_{pulse}\approx$ 15 ns (Spectron Laser Systems), are used. The laser beams are focused weakly onto the front surface of the film, so that the entire surface area of the film is homogeneously irradiated (spot area: 1.5×2.5 mm^2). Calculations, following absorption measurements on the samples, show that almost all the incident photons (99 %) of the UV wavelength (248 nm) are absorbed within a thickness of about 14.5 μm, and thus, all the photochromic transformations occur in these layers. The macroscopic contraction of the films is observed by recording their bending following pulsed-laser irradiation.

The bending of these photodriven switches is detected by monitoring the light of a cw He-Ne laser, which is deflected by the backside of the photochromic-polymer photoswitch. The spot diameter of the He-Ne laser beam on the film is 0.5 mm, and it is incident on the sample towards its freestanding edge at an incidence angle ~ 10-20˚ to the normal to the surface. A digital camera is used for monitoring the movement of the deflected beam on a graduated screen, simultaneously with the laser light irradiation. The graduated screen is located opposite to the sample and few tens of centimeters away.

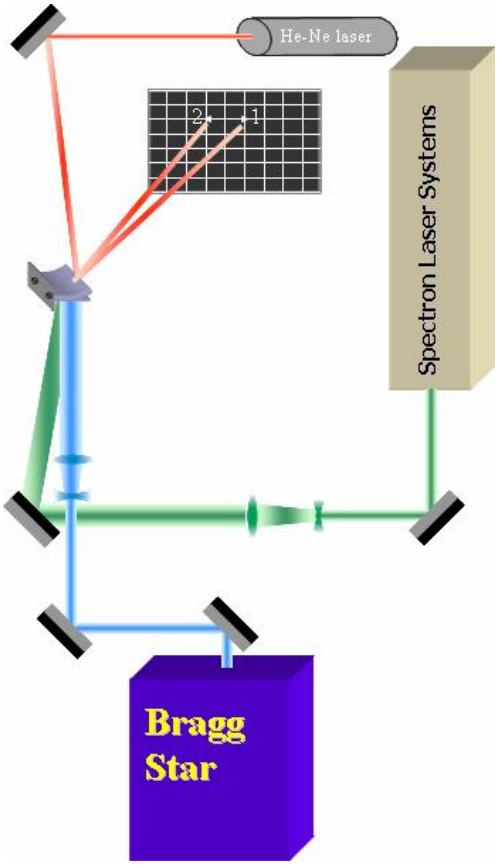

Figure 6.1.1.: Experimental set up for the beam deflection experiments.

6.2 Parameters affecting the magnitude of the volume change

As mentioned above, varying the parameters of the incident laser light can control the magnitude of the contraction of the polymer. An example is given in figure 6.2.1 where eight consecutive contraction-recovery cycles of a photochromic-polymer sample are presented, demonstrated by the reversible movement of the He-Ne laser beam deflected by the freestanding edge of the sample.

It is clearly demonstrated that an increase in the number of the incident UV pulses induces an increase to the contraction effect. In the first cycle of the experiment presented in figure 6.2.1 it can be seen that the deflection from the photochromic polymeric cantilever, does not move upon irradiation of the cantilever with just one UV pulse, indicating that no apparent dimensional change

occurs in the host matrix. Nevertheless, when the sample is irradiated with green pulses following the single UV pulse there is an obvious dimensional change of the polymer matrix. Upon continuous irradiation with green laser pulses the bended sample recovers eventually to its initial position.

In the next cycles presented in figure 6.2.1 where higher number of UV pulses is used it can be seen that the mechanical effect is already induced upon the use of UV pulses. The maximum displacement of the deflected beam, and thus the contraction of the sample reach a plateau after irradiation with more than 100 UV pulses. The magnitude of the maximum contraction of the sample in one dimension is found to be ~2.35 % of the initial length.

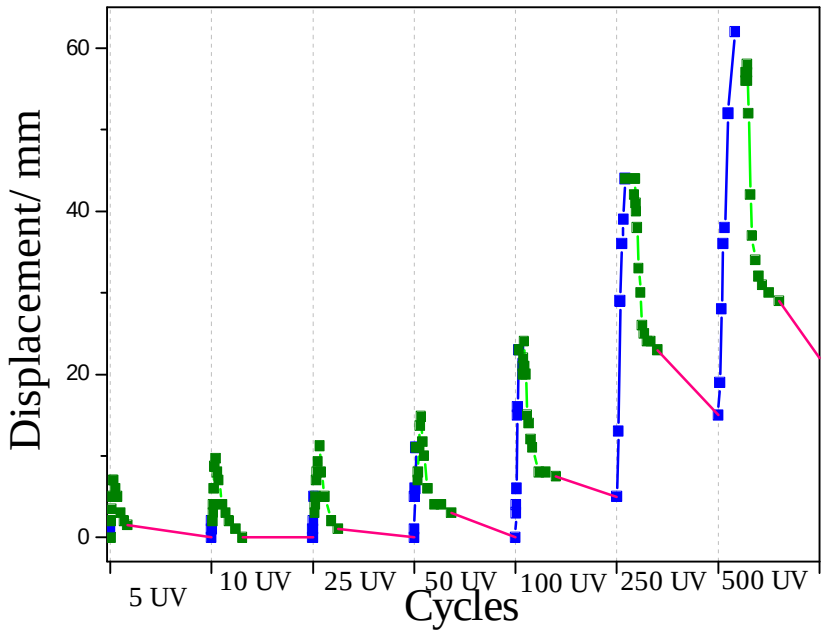

Figure 6.2.1: Eight successive contraction-recovery cycles of a photochromic-polymer sample of 5%SP-90%PEMMA.

6.3 Parameters affecting the speed of the volume change

In previous chapters, it has been extensively demonstrated that polymer substrates doped with SP molecules exhibit dimensional changes, induced exclusively by laser light. The beam deflection experiments clearly demonstrate

the act of these molecular substrates as photoswitches. For such a photoswitch to be used in real life, a high speed of operation is essential. For example a photoswitch used as a potential component for telecommunication equipments needs to operate at switching times suitable for the expanding traffic of telecommunication networks.

In the present chapter, an all-optically controllable photoswitch, capable of operating reversibly and with tunable speed, is presented. More specifically, it is examined how the parameters of the laser pulses that induce the forward and backward bending of the samples affect the switching time of this novel photoswitch. Two laser parameters are possible to affect the switching time by altering their values. The first deals with the frequency of the incident photons and the second one with number of photons in each pulse. The examined parameters are the repetition rate (number of pulses per time) and the fluence (energy per area).

It is already discussed in previous chapters that when UV laser pulses followed by green laser pulses irradiate the photochromic polymer film, it undergoes a mechanical cycle of macroscopic contraction and recovery. This mechanical response is converted into bending and unbending of the photochromic cantilever, due to the mechanism described in previous chapters. Green laser pulses are responsible exclusively for the complete bending cycle of the film used in these experiments, since the initial UV pulses are only used to induce the C-O bond breakage in the SP molecules and transform them to the MC isomers (SP→MC), process known as photocolouration.

Upon irradiation with the visible laser pulses, aggregates of some zwitterionic character stereoisomers are formed as a result of dipole-dipole interactions between the stereoisomers. As described in detail in the theory, these aggregates are found to be the photoproducts responsible for the macroscopic contraction and recovery of the examined samples. Subsequent irradiation with visible pulses reduces the number of MC stereoisomers since they are converted back to the SP form, and as a consequence, the number of the aggregates formed in each pulse is reduced. As the aggregates formation decreases the irradiated samples gradually return to their initial dimensions. The disappearance of the aggregates coincides with the recovery of the dimensions of the samples. According to the

above concisely described mechanism, a specific number of green pulses of certain energy is needed for the formation and disappearance of the aggregates and thus for the completion of the mechanical cycle.

Indeed, in Figures 6.3.1, 6.3.2, 6.3.3 it is clear that independently of the repetition rate of the laser pulses, each time a particular number of pulses is needed for the completion of the mechanical cycle, since their fluence is the same at each irradiation cycle. For example, despite the alteration of the repetition rate of the laser operating at 532nm from 10Hz to 30Hz, in each irradiation cycle 100 green pulses are necessary for the sample to return to its initial dimensions. This owes to the fact that a particular number of photons is required for the MC→SP transition which gradually results to the recovery of the film.

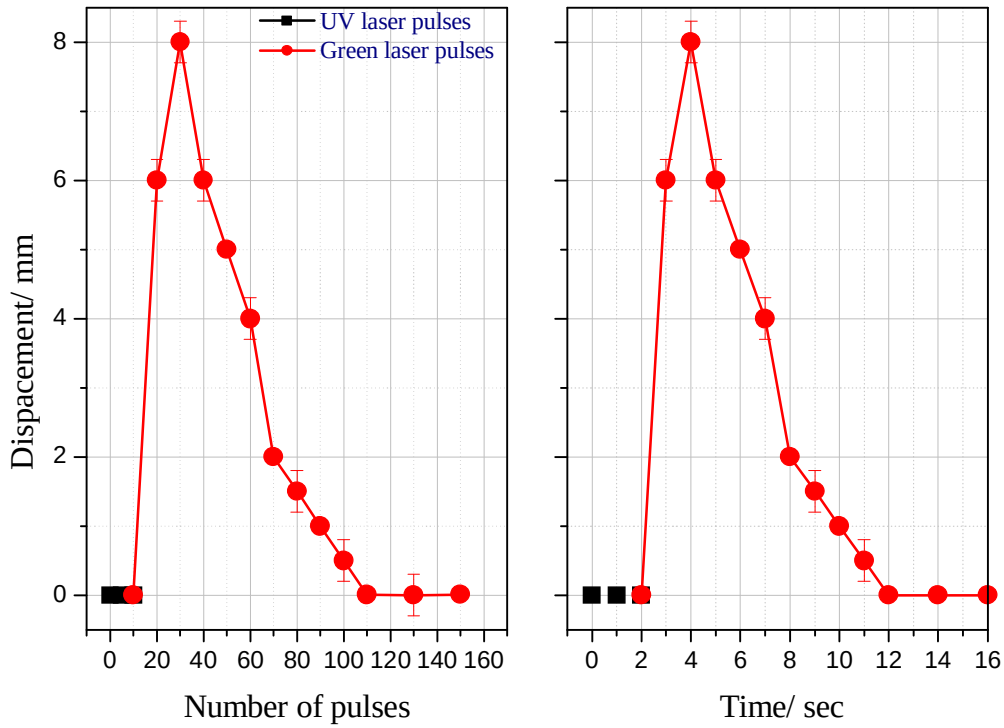

*Figure 6.3.1: Displacement of the deflected beam from the back surface of a 5%SP-90%PEMMA versus total number of pulses (left) and time (right) with **10Hz** repetition rate.*

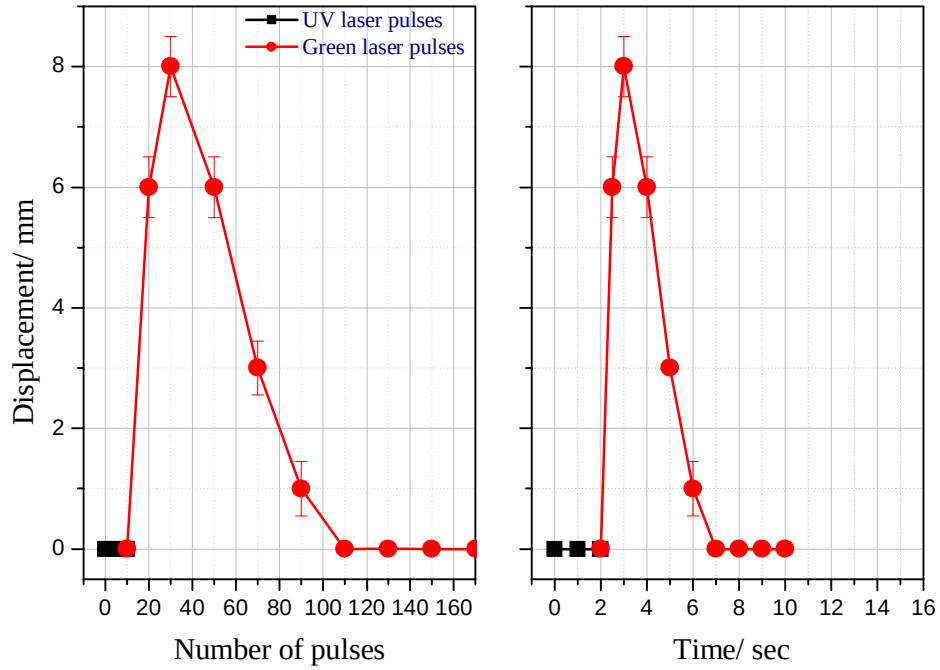

*Figure 6.3.2: Displacement of the deflected beam from the back surface of a 5%SP-90%PEMMA versus total number of pulses (left) and time (right) with **20Hz** repetition rate.*

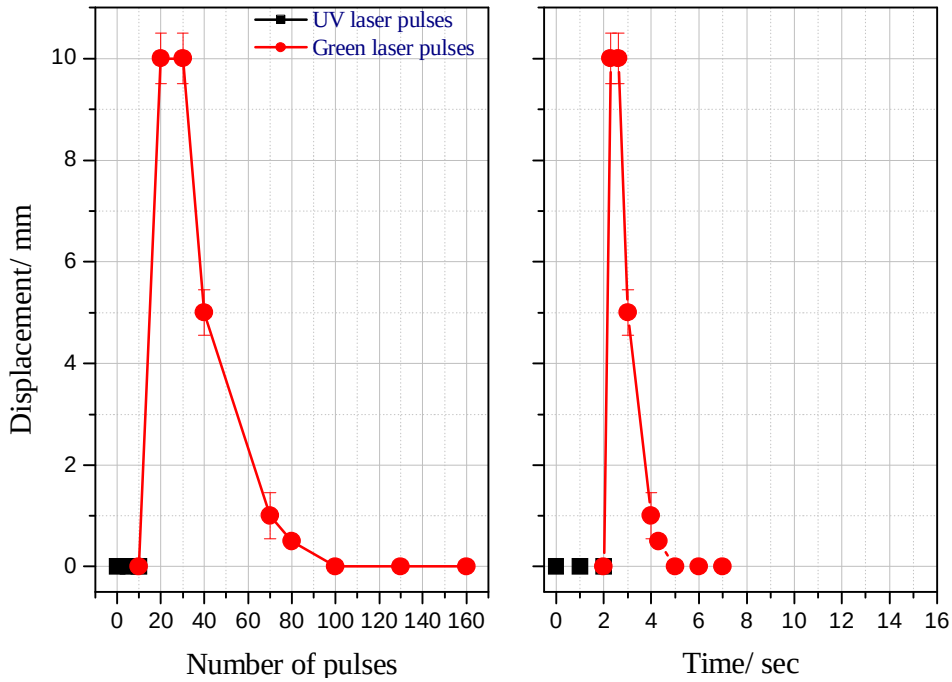

*Figure 6.3.3: Displacement of the deflected beam from the back surface of a 5%SP-90%PEMMA versus total number of pulses (left) and time (right) with **30Hz** repetition rate*

In the above figures the bending cycle of the photoswitch is represented by the displacement of the He-Ne laser beam, which is deflected from the backside of the photoswitch, as it undergoes the forward and backward bending. The displacement of the He-Ne beam is first plotted versus the number of green laser pulses (at left), and secondly versus the time (at right). As the number of the laser pulses needed for the completion of the switching procedure remains stable in each cycle, increase of the repetition rate makes the procedure faster.

In particular the displacement of the He-Ne laser beam deflected from the back surface of a 5.0% by wt. SP-doped PEMMA film, 90 μm thick is presented. The fluence of the UV pulses (248 nm, 15 ns) is 30 mJ·cm $^{-2}$ and their repetition rate is 5 Hz. The fluence of the visible pulses (532 nm, 15ns) is 80 mJ·cm $^{-2}$ and their repetition rate varies. Under these irradiation conditions the switching time was 12 seconds, when the green photons prostrated to the film with a frequency of 10 Hz (Figure 6.4.1). An increase in the repetition rate to 20 Hz reduced the switching time to the 7 seconds (Figure 6.4.2). Further increase of the laser frequency to 30 Hz results to a 5 second duration of the optomechanical cycle (Figure 6.3.3).

The five-second period is the fastest ever observed switching time in functional molecular substrates consisting of macromolecular chains combined with photochromic molecules. The investigation of similar systems includes different photochromic molecules, such as azobenzene and spiropyran, chemically attached to a variety of polymeric matrices [34-36, 38]. These systems have shown significant photoinduced reversible structural changes attributed to the isomerization process of the attached photochromic units. In particular, the interconversion between the photoisomers can either induce structural changes in the attached macromolecules, or move along with them the chain of the macromolecules on which they are attached. The above mechanisms possibly make the mechanical procedure slow (tens of seconds to hours) [36-38]. In the photoswitch presented here, further increase of the repetition rate above 40 Hz sometime lead to unwanted thermal effects.

The second parameter examined which is responsible for the reduction of the switching time of the cantilever is the effect of the green laser pulses fluence. In the experiments, presented in figures 6.4.4 and 6.4.5, the repetition rate remains stable and the only variable parameter is the laser fluence. An increase of the laser fluence simply means that greater number of photons will reach the film during each pulse. Therefore we expect that since a certain number of photons is essential for the mechanical cycle, an increase in the pulse fluence will result to a consequent diminish of the operating time.

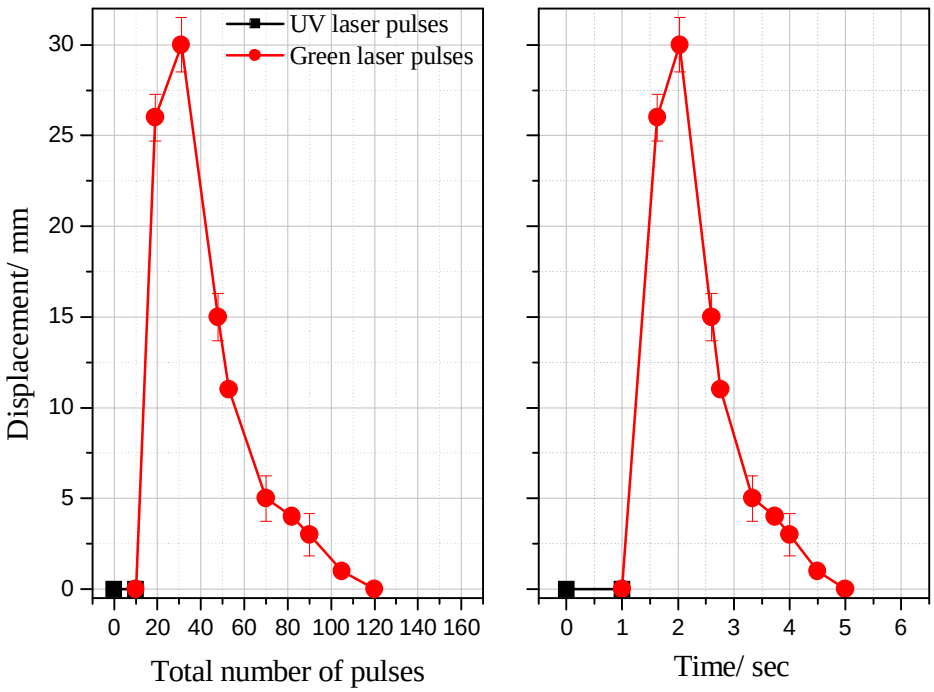

Figure 6.3.4: Displacement of the deflected beam from the back surface of a 5%SP-90%PEMMA versus total number of pulses (left) and time (right) for F_{green}*=80mJ/cm*^{2}*.*

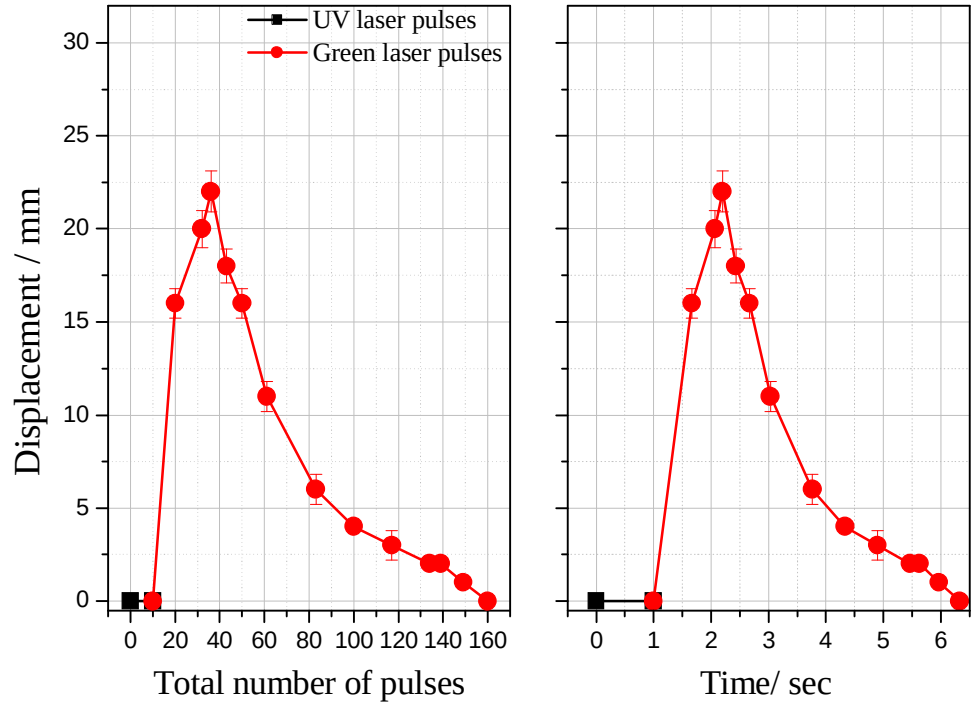

Figure 6.3.5: Displacement of the deflected beam from the back surface of a 5%SP-90%PEMMA versus total number of pulses (left) and time (right) for F_{green}*=65mJ/cm*^{2}*.*

Again, in figures 6.3.4 and 6.3.5 the forward and backward bending of the photoswitch is represented by the displacement of the He-Ne laser beam, deflected from its backside. The photoswitch used in the experiments presented in figures 6.3.4 and 6.3.5 is a 5.0% by wt. SP-doped PEMMA film, 35 μm thick. The fluence of the UV pulses (248 nm, 15 ns) is 35 mJ·cm^{-2} and their repetition rate is 10 Hz. The repetition rate of the green pulses (532 nm, 15ns) remains stable at all the cycles and is 30 Hz. Finally their fluence varies: In the first case presented in figure 6.3.4 it is 80 mJ·cm^{-2} and in the second case it is 65 mJ·cm^{-2} (Figure 6.3.5).

It is essential to mention here that the thickness of the sample forms no critical parameter for the switching time. Besides the larger displacement of the deflected beam due to the smaller residual volume that is dragged by the affected one, the optomechanical cycle will operate at the same time with a more bulk sample. This is explained by the fact that certain number of photochromic molecules needs certain number of photons in order to complete a cycle. Therefore even if it performs a greater forward and backward deflection the time needed for completion of the cycle will remain unaltered.

When the high fluence laser pulses were used, the bending and unbending of the sample was completed within 5 seconds, while in the case of the low fluence pulses the procedure became slower and it needed more than 6 seconds to be completed as presented in Figure 6.3.4.

As mentioned above, the dimensional variations of the samples involve formation and disappearance of MC dimers or complexes of higher stoichiometry. The phototransformations essential for the formation and disappearance of the aggregates is likely to need specific number of visible photons. Increase of the laser fluence implies increase of the number of photons in each laser pulse. Therefore less laser pulses are needed for the procedure to be completed and this is finally translated in faster photoswitches.

As demonstrated in figure 6.3.4 and 6.3.5, the laser fluence affects not only the speed of the mechanical cycle but also the magnitude of dimensional change of the samples. As the fluence of the green laser pulses increases the bending of the photoswitch becomes greater, and in as shown in figure 6.3.4 this is translated into larger displacement of the He-Ne beam deflected by the back surface of the photoswitch. Indeed, in figure 6.3.4 the displacement reaches the 30 mm whereas in figure 6.3.5, demonstrating the experiment where smaller fluence was used, the displacement decreases to 22 mm. This displacement reduction is translated in reduction of the maximum contraction of the samples by 0.1%. Therefore, it is obvious that by varying the fluence of the incident pulses the deflection of photoswitches can be very well adjustable.

To summarize, the polymer system PEMMA doped with Spiropyran photochromic molecules is investigated in the aspect of an operative photoswitch. It is demonstrated that varying specific parameters of the laser pulses can very well control the speed of the operation of this photoswitch. In particular use of higher repetition rates, leads to faster performances. Moreover the switching times of only few seconds are the shortest so far reported for similar photocontrollable systems consisting of macromolecular chains combined with photochromic molecules. Finally, the speed of the photoswitching procedure is affected by the fluence of the laser pulses. In particular, increase of the laser fluence makes the mechanical cycles faster. The laser fluence is also found to be an essential parameter, which can determine the magnitude of the dimensional changes of the switches. Hence,

the photoswitches presented here are tunable, since they can operate at variable speed and displacement by tuning the appropriate parameters of the lasers used for their operation.

7

“Smart” surfaces

7.1 Introduction

The overall increase in the development of polymeric materials for industrial applications deals with the mechanical properties of the bulk material as well as with the surface. The synthesis and study of nanostructured polymer systems designed to respond to external stimuli in a controlled and predictable manner has gain a great research interest due to uncountable applications of such materials (MEMS, microfluidic devices, switching of transport and separation, switching of viscosity, wetting, adsorption, and adhesion) [43]. Smart polymer surfaces are defined by the ability to change structure and properties when exposed to a particular stimulus in a controlled, reproducible, and reversible manner. Smart materials have the ability to switch their wettability, surface chemical composition, adhesive properties, etc. in controlled environment responding on the change of solubility, temperature, pH, etc. Little has been done to control the polymer response by using light. Design of materials with "smart" or "intelligent" behaviour

is of special interest. Such responsive polymers have many applications in diverse areas of research, including biology, telecommunications, and electronics.

7.2 Basic theoretical remarks for controlling the wettability of surfaces

.

Many processes in polymer production, development and application include wetting of solids by liquids. The wettability of a liquid is defined as the contact angle between a droplet of the liquid in thermal equilibrium on a horizontal surface. Contact angles of liquids on polymer surfaces are widely used to predict wetting and adhesion properties of these solids by calculating their solid-liquid surface tension. The theory is based on the equilibrium of an axisymmetric sessile drop on a flat, horizontal, smooth, homogeneous, isotropic, and rigid solid. Contact angle phenomena are very complicated. Contact angles on polymer surfaces are not only influenced by the interfacial tensions according to Young´s equation but also by many other phenomena, such as surface roughness, chemical heterogeneity, sorption layers, molecular orientation, swelling, and partial solution of the polymer or low-molecular constituents in the polymer material. These effects have to be considered when contact angle measurements are used to calculate the solid surface tension of polymers.

Final height and width of a water drop are determined only by surface energy of a liquid (surface tension), surface energy of the solid and gravity. Viscosity of the liquid affects the time elapsed until the drop finishes spreading.

$$s_L \cos q = s_S - s_{SL}$$ Young's equation

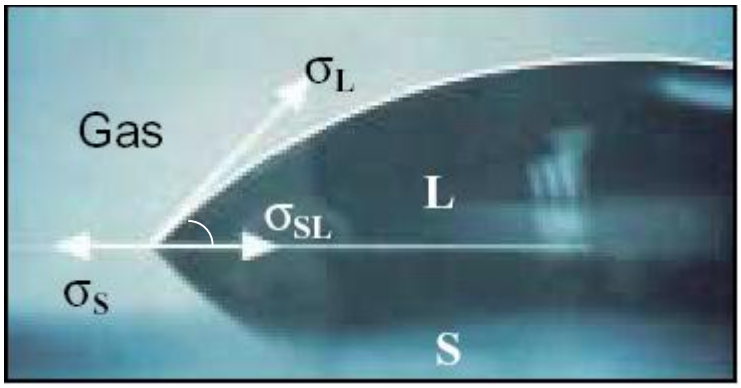

Figure 7.1: Surface tensions of a liquid droplet onto a solid surface.

Depending on the type of surface and liquid the droplet may take a variety of shapes as illustrated in figure. The wetting angle θ is given by the angle between the interface of the droplet and the horizontal surface. The liquid is seemed wetting when 90º<θ<180º and non-wetting when 0º<θ<90º. When θ=0º or θ=90º this corresponds to perfect wetting and the drop spreads forming a film on the surface.

Actually, the wetting angle θ is a thermodynamic variable that depends on the interfacial tensions of the surfaces**.**

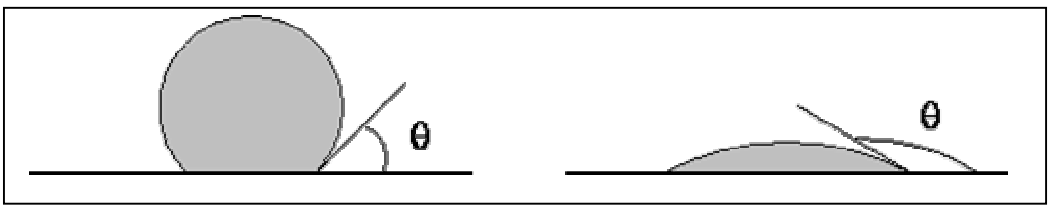

Figure 7.2: A liquid droplet in equilibrium with a horizontal surface surrounded by a gas. The wetting angle θ *between the horizontal layer and the droplet interface defines the wettability of the liquid. To the left: A non-wetting fluid with* 0º≤θ≤90º. *To the right: A wetting fluid with* 90º≤θ≤180º

7.3 Drop Shape Analysis

The shape of a liquid droplet on a solid surface is determined by a complicated interplay of the liquid surface tension, volume, density and contact angle. At equilibrium, an axisymmetric droplet obeys the Laplace Equation:

$$\Delta p = \gamma\left(\frac{1}{R_1}+\frac{1}{R_2}\right) \qquad (7.3.1)$$

in which (γ is the liquid surface tension, Δp is the pressure difference across the interface and R_1 and R_2 represent the two principal radii of curvature of the droplet and are given by the following relations.

$$\frac{1}{R_1} = \frac{\frac{d^2z}{dx^2}}{\left(1+\left(\frac{dz}{dx}\right)^2\right)^{\frac{3}{2}}} \qquad \frac{1}{R_2} = \frac{\frac{dz}{dx}}{x\left(1+\left(\frac{dz}{dx}\right)^2\right)^{\frac{1}{2}}} \qquad (7.3.2)$$

Where x and z are the Cartesian coordinates of each point in the profile of the drop. The strategy employed in the ADSA-P method is to construct an error function, which expresses the error between the measured curve and the numerically solved Laplace curve. This function is then minimised with a modified Newton-Raphson scheme. This strategy is necessary as the otherwise powerful Newton-Raphson method depends on a good initial approximation to the true curve.

The drop profile or the drop shape is dictated by a balance between the force of gravity, that is the buoyancy force, and the interfacial tension acting along the drop boundary. This balance is represented by various sets of differential equations that describe the drop profile. The dimensionless relationships for the drop geometry are typical of the above equations:

$$\begin{aligned} \frac{dq}{dS} &= \frac{2}{B} + \mathrm{Z} - \sin\left(\frac{q}{\mathrm{X}}\right) \\ \frac{d\mathrm{X}}{dS} &= \cos q \\ \frac{d\mathrm{Z}}{dS} &= \sin q \end{aligned} \qquad (7.3.2)$$

where X=cx, Z=cz, B=cb and S=cs are dimensionless variables defining the drop profile and c is the magnification factor defined by,

$$c^2 = \frac{(p_1 - p_2)g}{G} \qquad (7.3.3)$$

G is the interfacial tension, g is the gravitational constant, p_1 and p_2 are the densities of the drop fluid and the matrix fluid respectively, θ is the angle that the angle that the tangent to the drop profile at (X, Y) makes with respect to the

horizon and B is the shape parameter.tangent to the drop profile at (X, Y) makes with respect to the horizon and B is the shape parameter.

7.4 Experimental set up

To quantify wettability, thermodynamically relevant contact angles on smooth polymer surfaces are determined using a novel contact angle/ interfacial tension technique called Axisymmetric Drop Shape Analysis (ADSA) which is applicable not only for pendant and sessile liquid drops, but also for captive bubbles.

A schematic of the experimental set-up for ADSA-S sessile drop contact angle measurements is shown in figure 7.4.1.

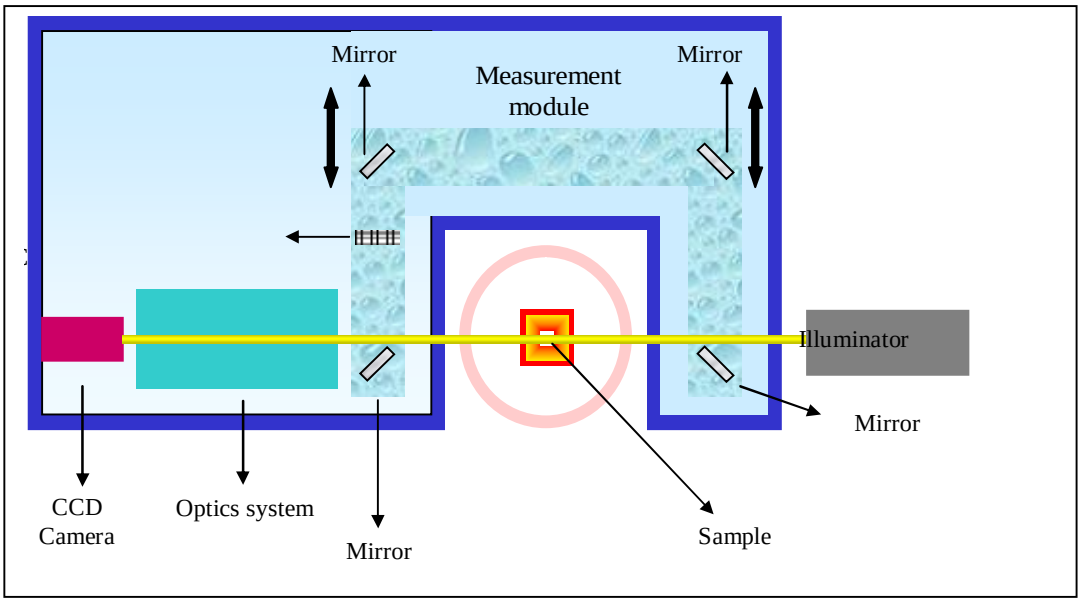

Figure 7.4.1: Experimental set up for ADSA-S [44].

The illuminator furnishes a variable intensity, monochromatic, collimated light source of homogenous brightness for lighting the drop image. The measurement module is a controlled environment chamber for formation of the sessile drop. The atmosphere must be a saturated vapor of the fluid phase. The optics system includes variable zoom optical components for magnification of the drop image and may also contain a reticle projection subsystem for the remote calibration of the optical magnification factor of the compound lens system.

Finally, a CCD camera is provided to record the video image, which is relayed to the frame grabber for digitisation.

7.5 Results

As discussed extensively in previous chapters the Spiropyran molecule upon irradiation in the UV region converts to its isomeric form called merocyanine. Merocyanine exhibits significant larger dipole moment compared to Spiropyran. When the C-O bond of the Spiropyran molecule in the pyran moiety breaks due to UV light absorption the electron pair of the bond follows the electronegative oxygen providing it with a negative charge. In the other hand due to formation of double bond between the carbon and the nitrogen the latter is provided with a positive charge as shown in figure 7.5.1.

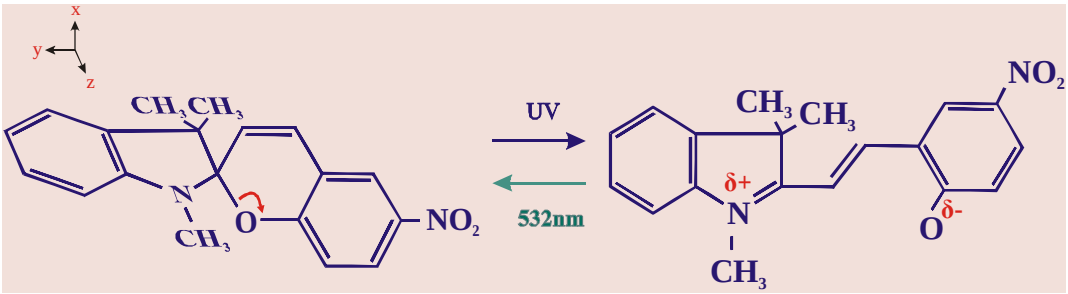

Figure 7.5.1: Spiropyran and the zwitterionic form of merocyanine

Thus we may rightly assume that upon UV irradiation a hydrophobic molecule such as Spiropyran is converted to a more hydrophilic one such as Merocyanine. By measuring the contact angle of water drop which lies onto the surface of the phorochromic polymer samples we quantify the wettability properties of the photochromic polymer surfaces. Increase in the contact angle means that the surface becomes more hydrophobic. Decrease in the contact angle simply means that the surface becomes more hydrophilic.

For the sessile drop measurements the samples were prepared with the spin coating method discussed in chapter 5.2. A UV laser operating at 308nm was used for the conversion of the Spiropyran to the merocyanine and a visible laser operating at 532nm for the back reaction. In the initial experiments the conversion of the merocyanine molecules to the spiropyran form was achieved by means of

heating. Nitrogen flow during the irradiation as well as the thermal procedure was used to prevent in way oxidation effects.

Three different pictures of the water drop were taken for each condition of the sample. One simultaneously after the setting of the drop onto the sample, one after five minutes and the final after ten minutes. The above procedure was followed in order for the system to reach its equilibrium point. To avoid the evaporation of the water drop the measurements were performed in humidity environment. Moreover in order to ensure that the water drop does not penetrate into the polymer surface we measured the contact angle every five minutes for a total interval of half an hour. No decrease in the value of the contact angle was observed until the first twenty minutes.

Initially we examined three different polymer sustrates to determine the role of the polymer matrix. We used polystyrene (100k) which is generally rigid, Poly ethyl methacrylate-co-methyl-acrylate (PEMMA) with T_g=48º and polymethylmethacrylate PMMA (100k) with T_g=100º. The first results which show the response of the polymeric surface to light exposure due to the presence of the photochromic dopants are presented in figures 7.5.1, 7.5.2, 7.5.3.

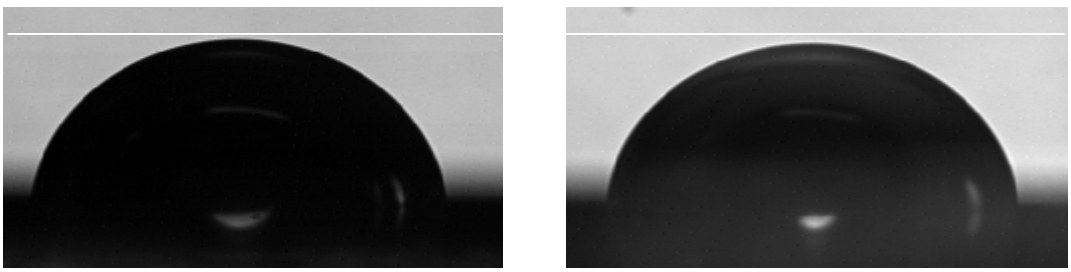

Figure 7.5.1: Water drops on a 10%SP-90%PS before (left) and after (right) 30 UV pulses of fluence 40mJ/cm^2

The contact angle was measured 84º before and 77º after the irradiation.

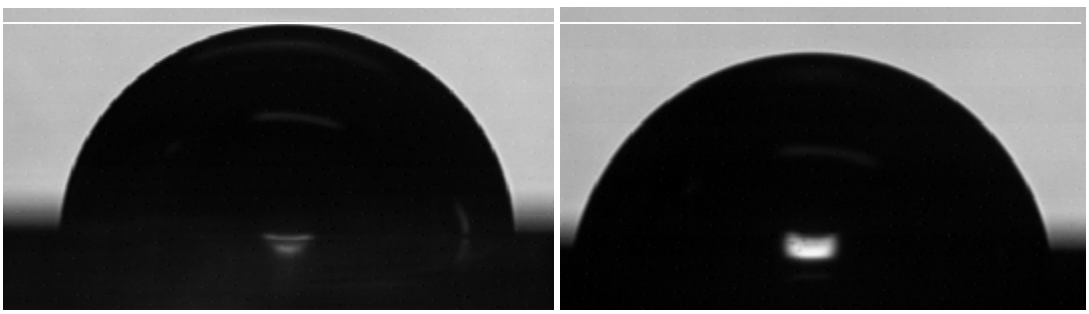

Figure 7.5.2: Water drops on a 10%SP-90%PEMMA before (left) and after (right) 30 UV pulses of fluence 40mJ/cm^2

The contact angle was measured 84º before and 74º after the irradiation.

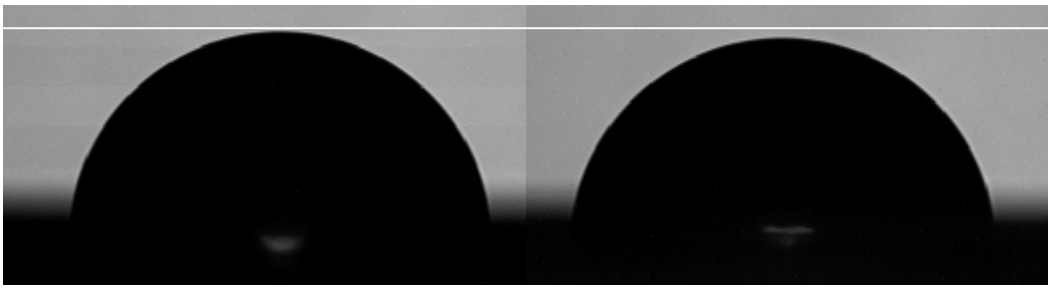

Figure 7.5.3: Water drops on a 10%SP-90%PMMA before (left) and after (right) 30 UV pulses of fluence 40mJ/cm^2

The contact angle was measured 84º before and 74º after the irradiation.

We clearly observe that each time the sample was irradiated with 30 UV pulses a decrease in the contact angle occurred for all the polymer matrices that we examined. In the case of PEMMA used as polymer matrix a larger decrease in the contact angle was observed. The above result deals with the rigidity of the polymer as well as with the surface tension properties. We may observe though that in the case of PEMMA used as polymer matrix the maximum decreas ein the contract angle was measured. Therefore samples of PEMMA doped with photochromic Spiropyran molecules will be used in the following experiments.

The next step was to examine the reversibility of the phenomenon. For this reason we heat the samples for twenty minutes sufficiently below the glass transition temperature. As previously reported heating is responsible for the conversion of the merocyanine molecules to the spiropyran form. The results are shown in figure 7.5.4.

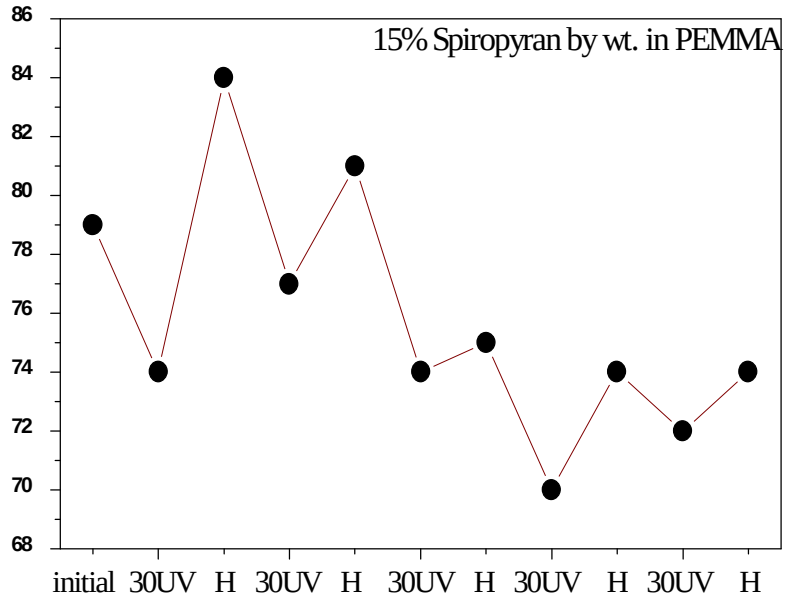

*Figure 7.5.4 : UV –Heating cycles for a 10% Sp-P*EMMA *sample*

From the above figure we observe that every time the sample is irradiated with UV pulses the contact angle decreases while every time it is heated the contact angle was increased not to the initial value though.

The above results indicate that heating does affect the samples. We can assume that it destroys them in a way. This is clear from the fact that the contact angle never converts to its initial value. Moreover we observe that it decreases in each irradiation cycle. For this reason we performed experiments were we used visible laser for the conversion of the samples along with a nitrogen flow to prevent oxidation as discussed in previous chapters. The results are shown in figures 7.5.5 and 7.5.6.

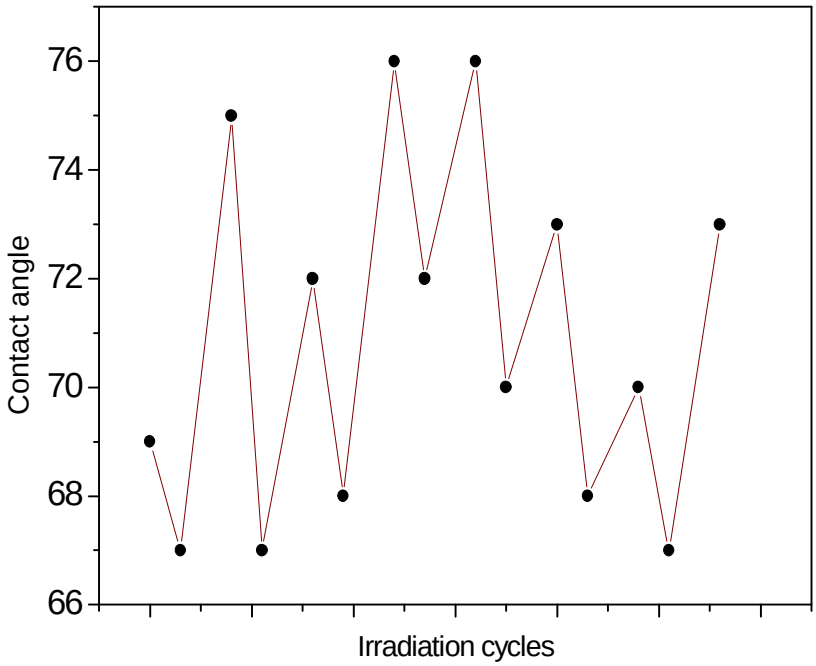

Figure 7.5.5 :UV –Vis cycles for a 5% Sp-PEMMA sample

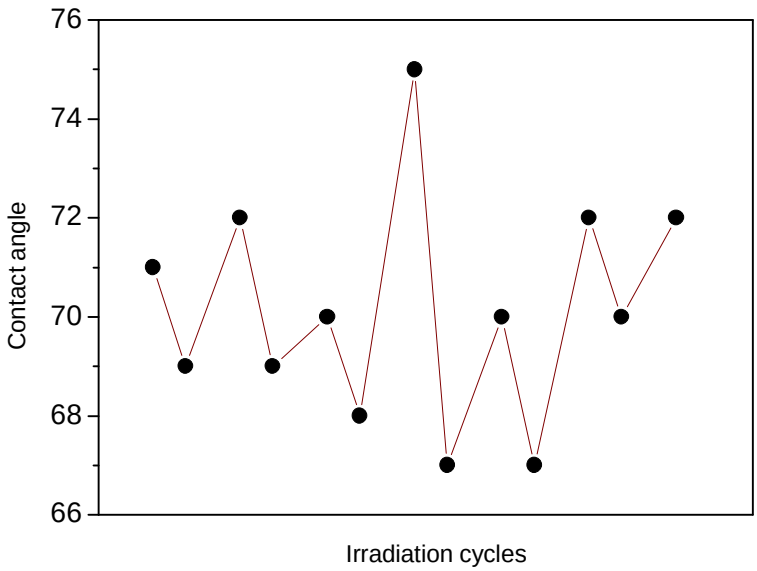

Figure 7.5.6 :UV –Vis cycles for a 10% Sp-PEMMA sample

In the above figure its time the sample is irradiated with UV pulses the contact angle decreases while its time visible light is absorbed the contact angle increases. So, with the use of visible laser a nice repentance of the phenomenon sounds promising. Further experiments are in progress in order to stabilize the difference in the contact angle.

7.6 Summary

Light responsive surfaces were presented in this chapter. Upon UV irradiation Spiropyran molecules are converted into its isomeric form called merocyanine. Merocyanine molecules exhibit a significant dipole character in contrast to the Spiropyran molecules. Thus the conversion of the Spiropyran to the merocyanine molecules can be used to convert surfaces form hydrophobic to hydrophilic. Water is a dipole molecule, which reacts to the presence of dipoles (merocyanine molecules). Therefore by measuring the contact angle of a water drop onto the photochromic polymer surfaces we study the wettability properties of the polymer surfaces. The use of lasers for the conversion of the Spiropyran molecule to its zwitterionic form Merocyanine makes the polymer surfaces light responsive. Further investigation takes place in order to increase the effect by using patterned surfaces. In the same time factors such as fluence or number of pulses are examined to elucidate their influence.

References:

[1] Fisher, E., Hirshberg, Y. *J., Chem. Soc*., 4522-4524, (1952).

[2] *Photochromism*, G. H. Brown (Ed.), Wiley-Intersciences, New York (1971).

[3] Bertelson, R. C, *Mol. Cryst. Liq. Cryst*. **246**, 1, (1994)

[4] Bouas-Laurent, H., Durr, H., *Organic photochromism* (IUPAC Technical Report).

[5] Parthenopoulos, D. A., Rentzepis, P. M, *Science*, **245**, 843, (1989)

[6] Dvornikov, A. S, *Optical Computing Hardware*, Ch. 11, AT&T and Acad. Press (1994)

[7] Crano, J. C., Guglielmetti, R. J. (eds) *Organic photochromic and Thermocromic compouns,* Vols.1 and 2. Plenum Press, New York.

[8] Dűrr, H., Bouas-Laurent, eds., *Photochromism: Molecules and Systems*, Elsevier Amsterdam (1990).

[9] Tyer,. Jr., N. W., Becker, R. S., *J. Am. Chem. Soc*., **8**, 145-165.

[10] Salemi-Delvaux, C., Luccioni-Houze, B., Baillet, G., Giusti, G. Guglielmetti, R. *J.Photochem. Photobio., A: Chem*, **91**, 223-232.

[11] Zhang, Schwartz, King, Harris :*J. Am. Chem. Soc.* **114**, 10921-10927 (1992).

[12] Wilkinson et al, *J. Chem. Soc*, **92**, 1331-1336 (1996).

[13] Ernsting, Arthen-Engeland :*J. Phys. Chem*. **95**, 5502-5509 (1991).

[14] Nakabayashi, T., Nishi, N., Sakuragi, H., *Science Progress*, **84,** 137-156 (2001).

[15] Yasuo Abe, Ren Nakao, : *J.Photochem. Photobio., A: Chem*. **95**, 209-214, (1996)

[16] Krongauz, V., Kiwi, J., *J. Photochem*, **13,** 89-97, (1980)

[17] Kalisky, Y, et al, *J. Phys. Chem*. **87**, 5333-5338 (1983)

[18] Lenoble, C., Becker, R., *J. Phys. Chem*. **90**, 62-65, (1986)

[19] Reeves, D., Wilkinson, F., *J. Chem. Soc*, **69**, 1381-1390 (1973)

[20] Krysanov, S., Alfimov, M., *Chem. Phys. Lett.*, **91**, 77-80, (1982)

[21] Görner, H. : *Phys. Chem. Chem. Phys.* **3**, 416-423 (2001)

[22] Chibisov, A. K., Görner, H. :*J. Phys. Chem. A,* **101**, 4305-4312 (1997)

[23] J. B. Flannery, J. Am. Chem. Soc. **90**, 5660, (1968)

[24] A.Athanassiou, K.Lakiotaki, V.Tornari, S.Georgiou, C.Fotakis, Appl. Phys. A., **76** (2003)

[25] A.Athanassiou, K.Lakiotaki, M.Kalyva, S.Georgiou, C.Fotakis, Las. Phys., **13,** (2003)

[26] Blair, H.S. and Pogue, H.I., , *Polymer*, **23** , 779 (1982)

[27] Gonzalez-De Los Santos, E.A., Lozano-Gonzalez, M.J.,and Johnson, A.F., *J.Appl.Polym.Sci.* , **71** , 259, (1999)

[28] A.Athanassiou, M.Kalyva, K.Lakiotaki, S.Georgiou, C.Fotakis, *Rev.Adv.Mat,* **5,** 245-251, (2003)

[29] Görner, H. :*Chem. Phys.* **222**, 315-329 (1997)

[30] K. Horie, K. Hirao, I. Mita, Y. Takubo, T. Okamoto, M. Washio, S. Tagawa, Y. Tabata, *Chem. Phys. Lett.*, **119**, 499, (1985)

[31] P. Uznanski, *Synthetic Met.*, **109,** 281, (2000)

[32] N. Angelini, B. Corrias, A. Fissi, O. Pieroni, F. Lenci, *Biophys. J.*, **74**, 2610 (1998)

[33] Y. Li, J. Zhou, Y. Wang, F. Zhang, X. Song, *J. Photochem. Photobiol. A*, **113** (1), 65 (1998)

[34] O. Pieroni, A. Fissi, N. Angelini, F. Lenci, *Acc. Chem. Res*, **34**, 9.(2001)

[35] A. Fissi, O. Pieroni, F. Ciardelli, *Biopolymers* 26, 1993 (1987**)**

[36] B. R. Malcolm, O. Pieroni, *Biopolymers*, **29**, 1121 (1990)

[37] T. Ikeda, M. Nakano, Y. Yu, O. Tsutsumi, A. Kanazawa, *Adv. Mater*, **15**, 201. (2003)

[38] Y. Yu, M. Nakano and T. Ikeda, *Nature* **425 (**2003), pp. 145.

[39] Heiligman-Rim, R., Hirshberg, Y., Fischer, E. *J. Phys. Chem*. **60**, 2465-2470 (1962)

[40] Bercovici, T., Heiligman-Rim, R., Fischer, E., *Mol. Photochem.*, **1**, 23, (1969)

[41] Takahashi, H., Yoda, K., Isaka, H., *Chem. Phys. Lett*., **140**, 90, (1987)

[42] Aldoshin, S., M., Atovmyan, L., *Mol. Cryst. Liq. Cryst*., **149**, 251, (1987)

[43] Anastasiadis, S., Retsos, H., Pispas, S., Hadjichristidis, N., Neophytides, S., *Macromolecules*, **36**, 1994-1999, (2003)

[44] Ρέτσος, Χ., Phd thesis, "*Μελέτη και τροποποίηση δομής και ιδιοτήτων επιφανειών-διεπιφανειών πολυμερών*", Πανεπιστήμιο Κρήτης, Τμήμα Φυσικής (2001).

[45] A. Athanassiou, M. Kalyva, K. Lakiotaki, S. Georgiou, C. Fotakis, *Adv. Mater.*. (to appear)